

## Design of crystal packings of styrylheterocycles and [2+2] photocycloaddition reactions in their single crystals

### 7.\* Crystal structures of 4-styrylpyridine hydroperchlorates and solid-state [2+2] autophotocycloaddition reactions of these compounds

L. G. Kuz'mina,<sup>a\*</sup> A. I. Vedernikov,<sup>b</sup> S. K. Sazonov,<sup>b</sup> N. A. Lobova,<sup>b</sup> A. V. Churakov,<sup>a</sup>  
E. Kh. Lermontova,<sup>a</sup> J. A. K. Howard,<sup>c</sup> M. V. Alfimov,<sup>b</sup> and S. P. Gromov<sup>b\*</sup>

<sup>a</sup>N. S. Kurnakov Institute of General and Inorganic Chemistry, Russian Academy of Sciences,  
31 Leninsky prosp., 119991 Moscow, Russian Federation.

Fax: +7 (495) 954 1279. E-mail: kuzmina@igic.ras.ru

<sup>b</sup>Photochemistry Center, Russian Academy of Sciences,  
7A-1 ul. Novatorov, 119421 Moscow, Russian Federation.

Fax: +7 (495) 936 1255. E-mail: spgromov@mail.ru

<sup>c</sup>Department of Chemistry, University of Durham,  
South Road, Durham DH1 3LE, UK

A series of 4-styrylpyridine hydroperchlorates were synthesized, and the [2+2] autophotocycloaddition (PCA) reaction in their polycrystalline films and single crystals resulting in the centrosymmetric *rect* isomers of 1,2,3,4-tetrasubstituted cyclobutanes was investigated. Unlike neutral styrylpyridines, their protonated forms are better preorganized for the solid-state PCA reaction. According to the X-ray diffraction data, the cations of these compounds, like related styryl dyes, are mainly stacked in crystals in a head-to-head or head-to-tail fashion with equal probability. Only in the latter type of stacks, the PCA reaction is feasible as a single-crystal-to-single-crystal transformation. The crystal packing is stabilized by hydrogen bonds between organic cations and perchlorate anions, as well as by other weak directional interactions, for example, by S...S interactions, thus preventing the atomic displacements in the course of PCA. The completion of the PCA reaction in single crystals without their degradation was observed only for 15-crown-5-containing 4-styrylpyridine hydroperchlorate. The crystals of the latter compound are stabilized not by hydrogen bonds between the cations and anions but by N<sup>+</sup>—H...O(macrocyclic) hydrogen bonds resulting in the formation of head-to-tail stacked dimers. In the crystals, these dimers are surrounded by a soft shell formed by rotationally and translationally mobile anions and benzene solvent molecules, as well as by conformationally flexible crown-ether moieties of adjacent dimer pairs. This leads to a decrease in the steric strain that occurs in the crystals in the course of PCA and prevents the degradation of single crystals. The PCA reaction is accompanied by the reduction in the crystal symmetry due to the doubling of the unit cell.

**Key words:** styrylheterocycles, X-ray diffraction study, crystal packings, design of crystal packings, solid-state [2+2] photocycloaddition, cyclobutanes, NMR spectroscopy.

The [2+2] photocycloaddition (PCA) reaction of unsaturated compounds giving cyclobutane derivatives, which was discovered in the beginning of the 20th century and then developed in 1960s,<sup>2–4</sup> continues to attract great interest,<sup>5–11</sup> because this reaction provides a simple and often the only possible approach to the synthesis of substituted cyclobutanes and can be used in optical data recording systems.<sup>12</sup> This reaction can take place in solutions, gels, and micelles, as well as between solids (in polycrys-

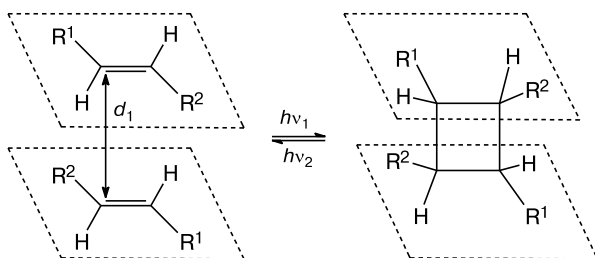
talline films and single crystals), under visible or UV irradiation of unsaturated compounds. Photoreactions that proceed as single-crystal-to-single-crystal transformations (*i.e.*, with the retention of the crystallinity of the sample) were documented;<sup>13–19</sup> however, the PCA reactions much more often result in the degradation of single crystals to form the amorphous (glassy) state or lead to substantial cracking of single crystals.

For the PCA reaction to occur, a particular spatial preorganization of two starting unsaturated molecules is required. Thus, the molecules should be arranged in paral-

\* For Part 6, see Ref. 1.

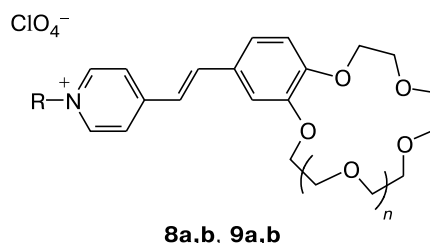
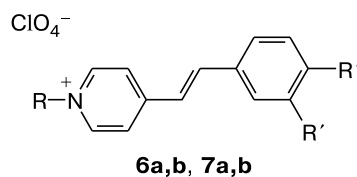
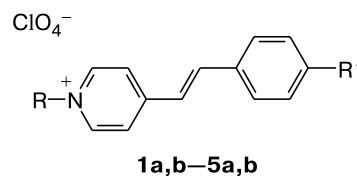
lel planes in such a way that their ethylene groups are located one above another and are oriented parallel (or antiparallel) to each other with the distance  $d_1$  between the carbon atoms varying in the range of 3.3–4.2 Å (Scheme 1). This preorganization can be provided by the crystal lattice (topochemical control). Hence, the solid-state PCA reaction proceeds, as a rule, stereoselectively, *i.e.*, only a few isomers or the only isomer of the cyclobutane derivative out of a large number of theoretically possible isomers are formed.

Scheme 1



Earlier,<sup>1,20–25</sup> we have studied the solid-state PCA reactions of styryl dyes of the general formula  $R-Het^+-CH=CH-Ar X^-$ , in which the quaternized nitrogen heterocycle is linked to the aryl moiety *via* an ethylene bridge, and  $X^-$  is the inorganic counterion, as well as the PCA reactions of their synthetic precursors, *viz.*, neutral styryl-heterocycles  $Het-CH=CH-Ar$ . Since PCA can proceed as the single crystal-to-single crystal reaction, it is evident that the crystal packing not only provides the preorganization of the structural units required for the reaction but also ensures the existence of the resulting cyclobutane structures within the starting crystals (*i.e.*, in the same space group, with the similar unit cell parameters, in the presence of inclusions of the unreacted starting molecules). For a large number of dyes belonging to 4-styrylpyridine (for example, **1a–9a**), 4-styrylquinoline, and 2-styryl-benzothiazole series, it was found<sup>20–25</sup> that these compounds form predominantly stacked architectures in the crystals (Fig. 1, **a** and **b**), in which the chromophoric moieties of adjacent molecules are projected onto each other, *i.e.*, the crystal lattice provides the preorganization of the structural units favorable for the PCA reaction. These packing motifs are not typical of the crystals of neutral styrylheterocycles.<sup>1</sup> The latter compounds tend to form ladder (**c**), ladder-herringbone (**d**), and sandwich packings, for example, sandwich-herringbone packings (**e**) (see Fig. 1).

Undoubtedly, there is a genetic relationship between the stacking (**a**, **b**) and non-stacking motifs (**c–f**). The motifs **c** and **d** are derived from the motifs **a** and **b**, respectively, by the equal shifts of each molecule of the stack in its own plane with respect to the previous molecule until



$R = Et$  (**a**),  $H$  (**b**);  $R' = H$  (**1**),  $NO_2$  (**2**),  $NMe_2$  (**3**),  $OMe$  (**4**, **6**),  $SMe$  (**5**),  $Cl$  (**7**);  $n = 1$  (**8**),  $2$  (**9**)

their mutual projection disappears. The motifs **e** and **f** are derived by the corresponding shifts of a pair of molecules (rather than of one molecule) in the packings **b** and **a**,

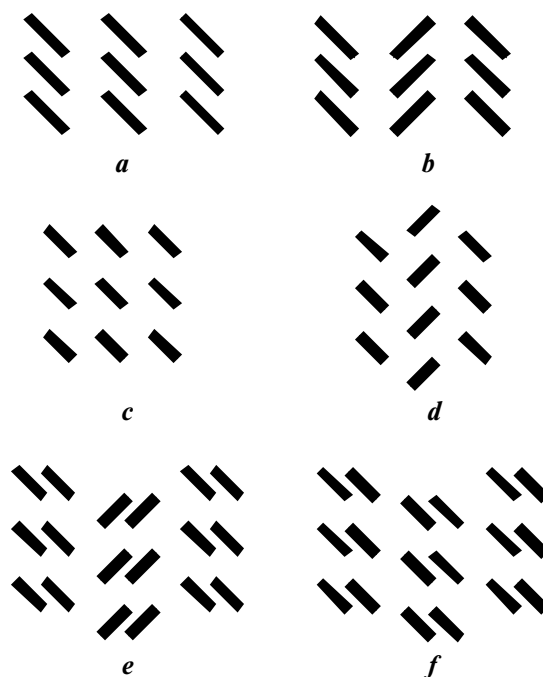


**Fig. 1.** Types of the crystal packings typical of styryl dyes (**a**, **b**) and neutral styrylheterocycles (**c–f**); the line segments represent the lateral projections of the  $\pi$ -conjugated systems.

respectively. The theoretically possible ladder-sandwich motif *f* has not been observed in the crystal packings of styryl dyes and neutral styrylheterocycles. Evidently, of the four packing motifs possible for the latter compounds, pairs of molecules (stacked dimer pairs) preorganized for the PCA reaction in single crystals can exist only in two sandwich motifs *e* and *f*, because chromophores are projected onto each other only in these motifs.<sup>1,22</sup>

The aim of the present study was to modify neutral styrylheterocycles in such a way that the formation of the packing motifs *e* and *f* or even the transformation to the stacking motifs *a* and *b* would be favorable. In the previous paper,<sup>1</sup> we have described our first approach to the crystal design of these compounds. This approach is based on the extension of the  $\pi$ -conjugation region in the molecules, which increases the probability of the appearance of stacked elements (dimer pairs) in the crystal packing. In the present study, we developed an alternative approach based on the use of protonated forms of styrylheterocycles,  $\text{H-Het}^+-\text{CH}=\text{CH}-\text{ArX}^-$ , which can be easily prepared by the treatment of neutral styrylheterocycles with strong mineral acids. We chose  $\text{HClO}_4$  as the mineral acid because it has earlier been shown<sup>20,23,24</sup> that perchlorate anions are favorable for the solid-state PCA reaction of styryl dyes, including single-crystal-to-single-crystal reactions. The external shape and the electronic structure of protonated styrylheterocycles are similar to those of the corresponding styryl dyes. Hence, it would be expected that the crystal packings of styrylheterocycles would be similar to those of styryl dyes, *i.e.*, styrylheterocycles would primarily form stacks.

It should be noted that the stereoselective PCA reactions of protonated styrylheterocycles in solution were documented,<sup>26–33</sup> including the reactions in the presence of macrocyclic compounds (cucurbit[8]uril,  $\gamma$ -cyclodextrin, calix[*n*]arenes);<sup>34–38</sup> however, the corresponding solid-state photoreactions are poorly known and were not systematically studied.<sup>26,39</sup>

In the present study, we report the synthesis and results of the X-ray diffraction study of 4-styrylpyridine hydroperchlorates **1b–9b** and analyze their crystal packings. Single crystals were irradiated with visible light. The crystals, which did not crack and were not transformed into the amorphous state, were repeatedly studied by X-ray diffraction. To confirm the occurrence of the solid-state PCA reaction and its stereochemical result, we also irradiated polycrystalline films of compounds **1b–9b** and analyzed the photoproducts by  $^1\text{H}$  NMR spectroscopy.

## Results and Discussion

Hydroperchlorates **1b–9b** were synthesized by the reaction of the corresponding neutral (*E*)-4-styrylpyridines with 70% perchloric acid. The resulting salts were characterized by UV and  $^1\text{H}$  NMR spectroscopy and elemental

analysis. The absorption spectra of compounds **1b–9b** are similar to the spectra of related dyes **1a–9a** (see Ref. 23 and the Experimental section), which confirms the similarity of the  $\pi$ -electron structures of these compounds.

Compounds **1b–9b** in the form of polycrystalline films on glass substrates were irradiated with visible light under comparable conditions. The compositions of the samples thus obtained were analyzed by  $^1\text{H}$  NMR spectroscopy. The results are given in Table 1. It should be noted that, although the films were prepared with the use of solutions of the compounds in a MeCN–benzene mixture, the signals of these solvents were observed in the  $^1\text{H}$  NMR spectra only in trace amounts. This indicates that the solvent molecules were relatively rapidly evaporated from the films upon heating with a closely placed incandescent lamp, which was used as the light source.

Compounds **3b**, **4b**, and **6b** proved to be insensitive to light. By contrast, the irradiation of compounds **1b**, **5b**, **8b**, and **9b** resulted in the formation of centrosymmetric *rect* isomers of cyclobutane derivatives **10**, **12**, **13**, and **14** (Scheme 2). The  $^1\text{H}$  NMR spectra of the latter compounds show characteristic<sup>20,22,23</sup> signals of cyclobutane protons at  $\delta$  5: two symmetrical doublets of doublets and the AA'BB'-type spin system (see, for example, Fig. 2). This is indicative of the existence of *syn*-head-to-tail stacked dimers in the solid state, which should precede the formation of cyclobutanes with this stereochemistry. The rates of the PCA reactions are substantially different. The photo-

**Table 1.** The starting styrylpyridine (SP)-to-cyclobutane (CB) derivative ratio and the degree of conversion ( $\chi$ ) in polycrystalline films of compounds **1b–9b** irradiated with visible light

Compound	<i>t</i> /h <sup>a</sup>	SP : CB <sup>b</sup> (mol/mol)	$\chi$ <sup>b</sup> (%)
<b>1b</b>	20	1 : 10.2	95
	50	0 : 1	100
<b>2b</b>	20	1 : 0.02	5
	140	1 : 0.57	53
<b>3b</b>	50	1 : 0	0
<b>4b</b>	70	1 : 0	0
<b>5b</b>	20	0 : 1	100
<b>6b</b>	80	1 : 0	0
<b>7b</b>	20	1 : 0.04 <sup>c</sup>	7
	140	1 : 0.06 <sup>c</sup>	11
	20	1 : 0.66	57
<b>8b</b>	20	1 : 0.66	57
	80	1 : 4.2	89
	200	1 : 8.6	95
<b>9b</b>	20	0 : 1	100

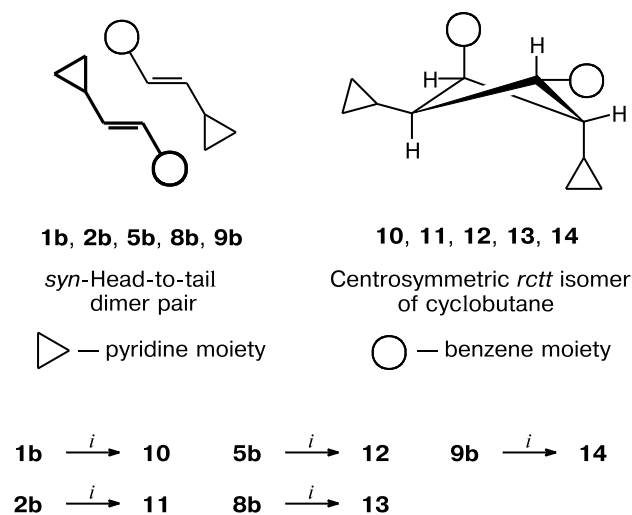
<sup>a</sup> The duration of irradiation.

<sup>b</sup> Based on the  $^1\text{H}$  NMR spectroscopic data.

<sup>c</sup> The reaction affords a mixture of two *rect* isomers of cyclobutane, which corresponds to the PCA reaction proceeding in the *syn*-head-to-tail and *syn*-head-to-head dimers, in a ratio of ~2 : 1.

transformation proceeds most rapidly in styrylpyridines **1b**, **5b**, and **9b** (almost quantitatively within 20 h), whereas the complete conversion of crown-containing compound **8b** was not achieved even within >200 h. In films of nitro and dichloro derivatives **2b** and **7b**, the PCA reaction proceeds slowly (the degree of conversion was 53 and 11%, respectively, after 140 h) and with lower stereoselectivity; in the case of **7b**, a mixture of two *rectt* isomers of cyclobutane is formed, for which the cations in the starting dimers should be arranged in a *syn*-head-to-tail and *syn*-head-to-head fashion.

Scheme 2



*i. hv*, in the solid state

On the whole, the behavior of protonated styrylpyridines **1b–9b** substantially differs from that of the corresponding styryl dyes **1a–9a**. The stereospecific PCA reaction proceeds relatively rapidly (the degree of conversion was 85–92% within 10 h) in the case of dyes **4a–6a**, **8a**, and **9a** containing electron-releasing alkoxy or meth-

ylsulfanyl groups in the benzene ring to form the centrosymmetric *rectt* isomers of cyclobutanes.<sup>23</sup> This is associated with the motif **b** (see Fig. 1, the cations stacked in a *syn*-head-to-tail fashion) in the crystal packing and the fact that these dyes show intense absorption in the visible region, which facilitates the fast phototransformation under visible light irradiation. In the case of dye **1a** containing the unsubstituted benzene ring and dyes **2a** and **7a** containing electron-withdrawing substituents, the PCA reactions are much slower. The reactions of **2a** and **7a** proceed also with lower stereoselectivity and give mixtures of two isomeric cyclobutane derivatives corresponding to the cycloaddition in *syn*-head-to-tail and *syn*-head-to-head dimer pairs. These results correlate well with the shift of the long-wavelength absorption maximum of these dyes to the near-UV region compared to the corresponding characteristics of dyes **4a–6a**, **8a**, and **9a** and, apparently, with a larger diversity of the packing motifs in the crystals of **2a** and **7a**. Like compound **3b**, dye **3a** containing the dimethylamino group in the benzene ring was not involved in the PCA reaction. Apparently, this is the common feature of compounds having this structure due both to the efficient conjugation between the highly electron-donating nitrogen atom of the substituent and the styryl chromophore and the packing mode of the molecules in the crystals.<sup>23,24</sup>

The above-mentioned differences in the behavior of protonated styrylpyridines **1b–9b** and the corresponding styryl dyes are difficult to explain without the consideration of the mutual orientation of the molecules in the solid state. Hence, we studied the crystal packings of these compounds.

**Structural features of the formula units in the crystals of compounds 1b–9b.** Single crystals of compounds **1b–9b** were grown according to two procedures. In one method, an excess of 70% perchloric acid was added to an acetonitrile solution of the corresponding neutral 4-styrylpyridine (or the previously synthesized individual compounds **1b–9b** were used), and the resulting solution was saturated with a benzene or EtOAc vapor in the dark. Another method was based on the crystallization of an equimolar mixture of styrylpyridine and transition or heavy metal perchlorate under the same conditions (see below). The structures of the formula units in the crystals of compounds **1b–5b** are shown in Fig. 3.

Compound **4b** crystallizes in two modifications: without solvent molecules or with the inclusion of benzene molecules if benzene is present in a mixture of the solvents. In the structures of **1b**, **3b**·0.5C<sub>6</sub>H<sub>6</sub>, and **4b**·0.5C<sub>6</sub>H<sub>6</sub>, the molecular cations are disordered over two positions related to each other by the rotation by 180° about the long axis. This disorder is a consequence of the temperature-dependent solid-state bicycle-pedal isomerization in the crystals,<sup>40,41</sup> when the ethylene group is rotated around single bonds and the aromatic substituents are only slight-

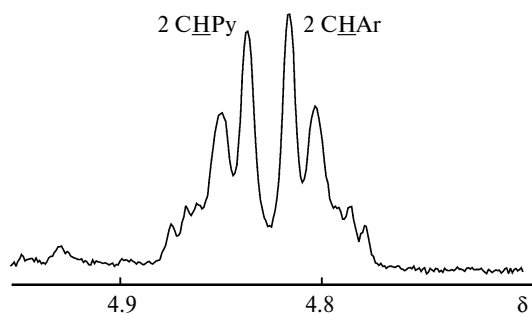


**Fig. 2.** <sup>1</sup>H NMR spectrum (DMSO-*d*<sub>6</sub>, 25 °C, the region of cyclobutane protons) of the photoproduct (*rectt* isomer **12**) prepared as a polycrystalline film by irradiation of compound **5b** for 20 h.

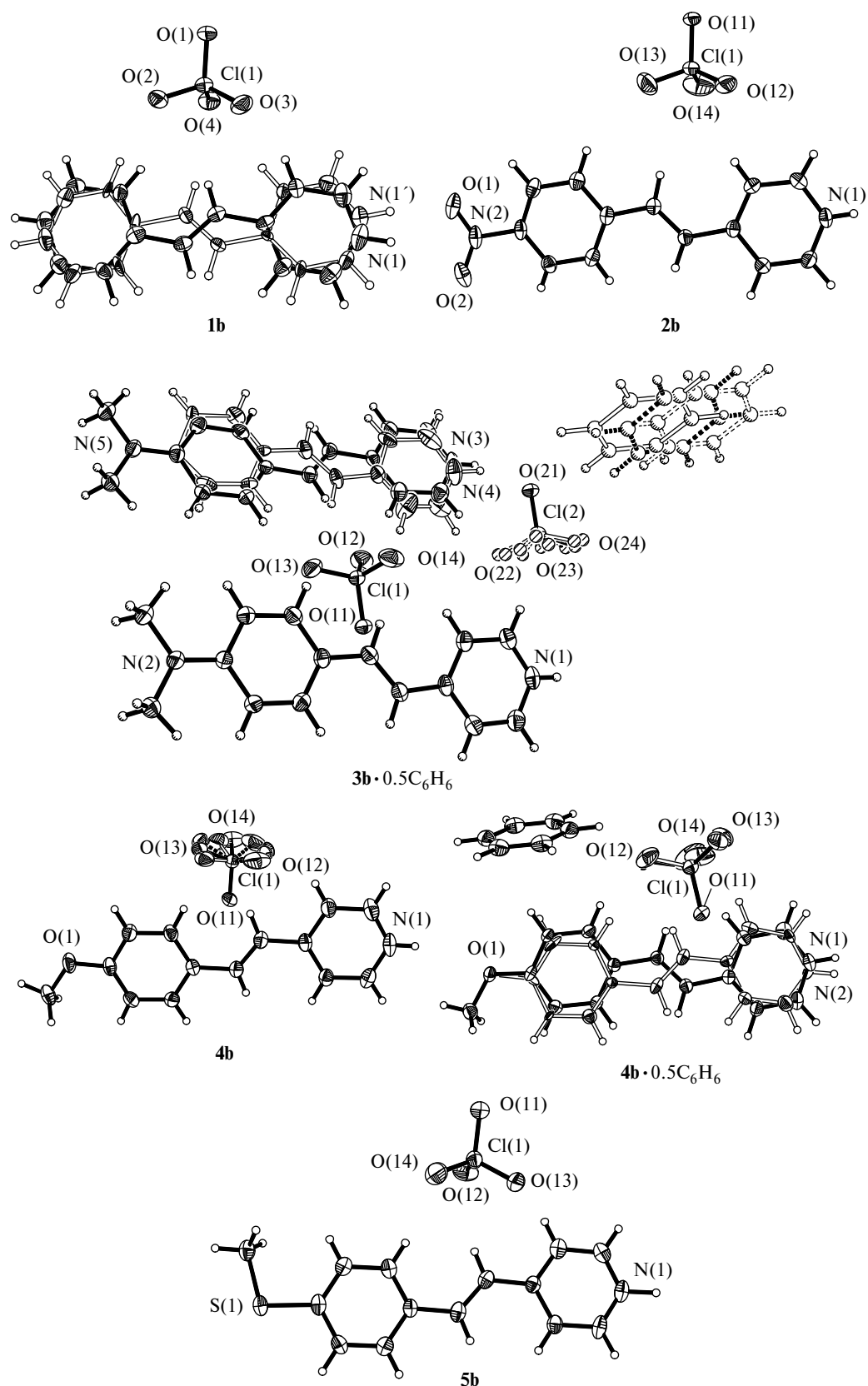


**Fig. 3.** Structures of the formula units in the crystals of **1b** (two *s* conformers), **2b**, **3b**·0.5C<sub>6</sub>H<sub>6</sub> (two independent molecules of **3b**, one of them as two *s* conformers, and the disordered benzene molecule), **4b**, **4b**·0.5C<sub>6</sub>H<sub>6</sub> (two *s* conformers), and **5b**. The nonhydrogen atoms are shown as displacement ellipsoids at the 50% probability level (except for the disordered benzene molecule in the structure of **3b**·0.5C<sub>6</sub>H<sub>6</sub>).

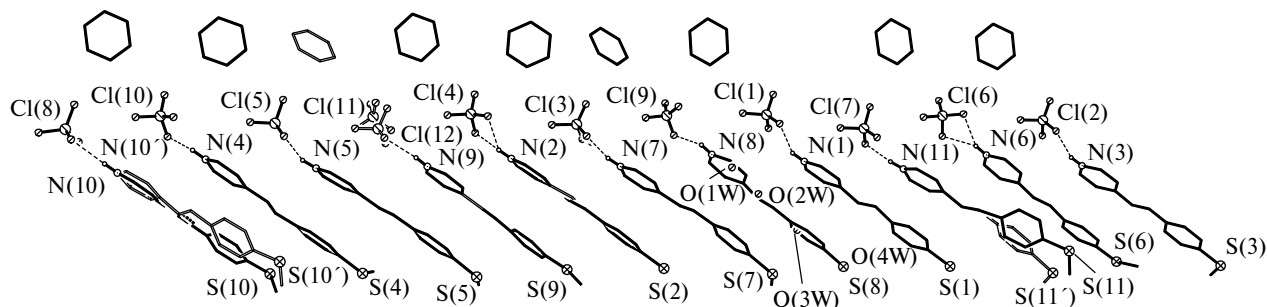


**Fig. 4.** Structures of the formula units in the crystal of  $5b \cdot 0.76C_6H_6 \cdot 0.14H_2O$  (11 independent molecules of  $5b$ ). The hydrogen bonds are shown as dashed lines.

ly shifted in their own planes. The occupancy ratio for the bicycle-pedal *s* conformers in the structures of **1b** and **4b**  $\cdot 0.5C_6H_6$  is 0.75 : 0.25 and 0.80 : 0.20, respectively. In the structure of **3b**  $\cdot 0.5C_6H_6$ , there are two independent molecules **3b**. One of them exhibits bicycle-pedal disorder with the occupancy ratio of the *s* conformers equal to 0.73 : 0.27, whereas another molecule is ordered. The benzene solvent molecule in this structure is disordered over three positions with the occupancy ratio of 0.50 : 0.25 : 0.25 (the displacement in the own plane). The perchlorate anions in the structures of **3b**  $\cdot 0.5C_6H_6$ , **4b**, and **4b**  $\cdot 0.5C_6H_6$  are disordered (rotation about one of the Cl—O bonds).

The crystals of compound **5b** were obtained as two triclinic crystal modifications. In one of them (see Fig. 3), solvent molecules are absent, whereas the composition of another modification is described by the formula  $5b \cdot 0.76C_6H_6 \cdot 0.14H_2O$ . We unexpectedly obtained crystals of the latter modification from a solution containing methylsulfanylstyrylpyridine and  $Ni(ClO_4)_2$  in attempting to grow crystals of the corresponding coordination compound. In the triclinic unit cell of  $5b \cdot 0.76C_6H_6 \cdot 0.14H_2O$ , there are 11 independent styrylpyridine molecules (Fig. 4). In some molecules, the central moiety is disordered, whereas the methylsulfanylbenzene moiety is disordered in other molecules, the latter being alternatively replaced by benzene solvent molecules. In the unit cell, there are also eight benzene solvent molecules with full occupancy. One of the styrylpyridine molecules occupies the position with half occupancy, and it is alternatively replaced by several water molecules. One of perchlorate anions is disordered over two closely spaced positions.

These X-ray diffraction data were collected from a weakly diffracting crystal, which has a very poor quality due to a too large fraction of disorder elements and contains a huge number of independent formula units. Undoubtedly, the structures of these imperfect crystals more precisely describe supermolecules self-organized in solution compared to the ideal crystal structures. These supermolecules have a structure (order), but the latter is less well organized and more loose than crystal structures.<sup>42</sup>

The investigation of these structures by X-ray diffraction is of great importance from the point of view of the further development of supramolecular chemistry. However, it should bear in mind that the low quality of X-ray diffraction data is an inherent property of these systems; the quality of these data cannot be substantially improved.

The structures of the formula units in the crystals of compound **6b** are shown in Fig. 5. Compound **6b** forms

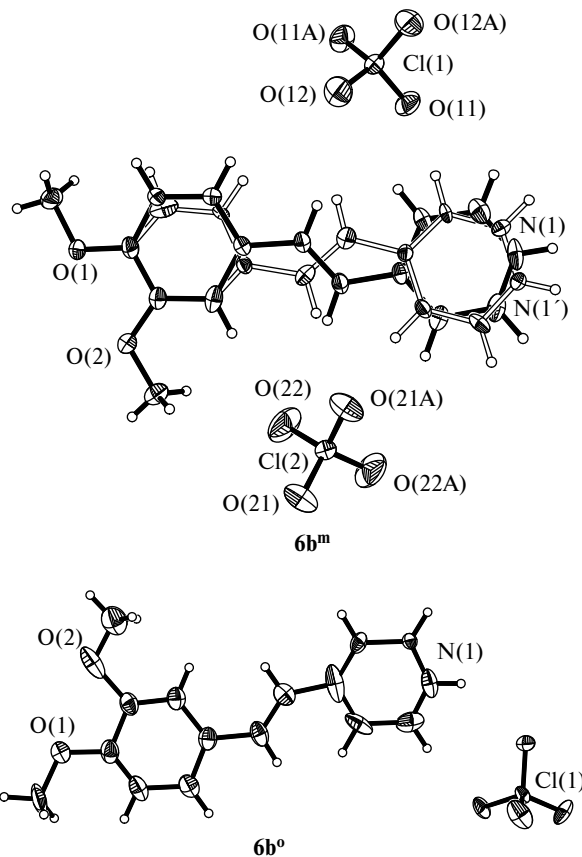


**Fig. 5.** Structures of the formula units in the crystals of  $6b^m$  (two *s* conformers) and  $6b^o$ . In the structure of  $6b^m$ , the atoms of the perchlorate anions labeled with A are related to the unlabeled atoms by symmetry operations.

two crystal modifications, *viz.*, monoclinic (**6b<sup>m</sup>**) and orthorhombic (**6b<sup>o</sup>**). The monoclinic modification was found in attempting to cocrystallize neutral dimethoxystyrylpyridine with the salts  $\text{Zn}(\text{ClO}_4)_2$ ,  $\text{Pb}(\text{ClO}_4)_2$ , or  $\text{Cr}(\text{ClO}_4)_3$ . Evidently, transition and heavy metal perchlorates are relatively easily hydrolyzed in the course of the crystal growth, and styrylpyridine is protonated by perchloric acid that is eliminated. Apparently, the presence of the above-mentioned salts facilitates the nucleation and growth of only the monoclinic modification, although the salts are not included in the growing crystal as components. In the crystals of **6b<sup>m</sup>**, the cation is distributed between two positions corresponding to the bicycle-pedal disorder with the occupancy ratio of 0.75 : 0.25. Two perchlorate anions occupy special positions on twofold axes. In the orthorhombic modification of **6b<sup>o</sup>**, the bicycle-pedal disorder also apparently takes place, as evidenced by the elongated thermal ellipsoids of the atoms as potential participants of this process, the relatively high R factor, and the presence of relatively high residual electron density peaks in difference Fourier maps in the region of the ethylene bond. However, this fact cannot be conclusively established because of the insufficiently high quality of the experimental data and the low content of the second *s* conformer. It should also be noted that this crystal is a racemic twin.

The crystal of **7b**·0.5C<sub>6</sub>H<sub>6</sub> contains eight molecules of the dichlorostyrylpyridinium salt and four benzene solvent molecules per asymmetric unit (Fig. 6). Like **5b**·0.76C<sub>6</sub>H<sub>6</sub>·0.14H<sub>2</sub>O, this structure is an example of a "loose" supramolecular assembly with a large number of structural units.

In the crystal of protonated 15-crown-5-containing styrylpyridine **8b** (Fig. 7), there are two crystallographically independent molecules of the major component, two

benzene solvent molecules occupying sites with half occupancy, and two water molecules with occupancies of 0.125, which are substantially disordered in the vicinity of centers of symmetry. Independent molecules **8b** form a pseudocentrosymmetric dimers. It is interesting that only one molecule in the dimer shows bicycle-pedal disorder in the form of two *s* conformers with almost equal occupancies (0.53 : 0.47). The position of another molecule is rigidly fixed. This is indicative of the difference in the crystal environment of the independent molecules. Thus, the environment of the "upper" molecule is looser because it allows it to be slightly shifted in the course of the dynamic bicycle-pedal isomerization, whereas the crystal environment of the "lower" molecule fixes it in the only possible position.

In this crystal, both independent perchlorate anions are also disordered (top and pendulum models).

Finally, two types of crystals were obtained for compound **9b**. In one of them, **9b** crystallizes as a solvate with acetonitrile and benzene molecules. In another type of crystals, **9b** crystallizes as a complex with ammonium perchlorate.

In the structure of **9b**·MeCN·0.5C<sub>6</sub>H<sub>6</sub>·H<sub>2</sub>O (Fig. 8), a part of the macrocycle distant from the benzene ring is disordered over two positions with the occupancy ratio of 0.68 : 0.32. The organic solvent molecules are also substantially disordered due, apparently, to the relative "looseness" of the crystal packing, as indirectly evidenced by the rapid degradation of the single crystals in air due to erosion. The water molecule is encapsulated in the cavity of the 18-membered macrocycle and forms hydrogen bonds with the oxygen atoms of the macrocycle: the O(1W)H...O(1)/O(6) bifurcated hydrogen bond (H...O, 2.20 and 2.37 Å; the angles at the H atom, 155 and 136°) and the O(1W)H...O(4) single hydrogen bond characterized by the parameters 2.11 Å and 173°.

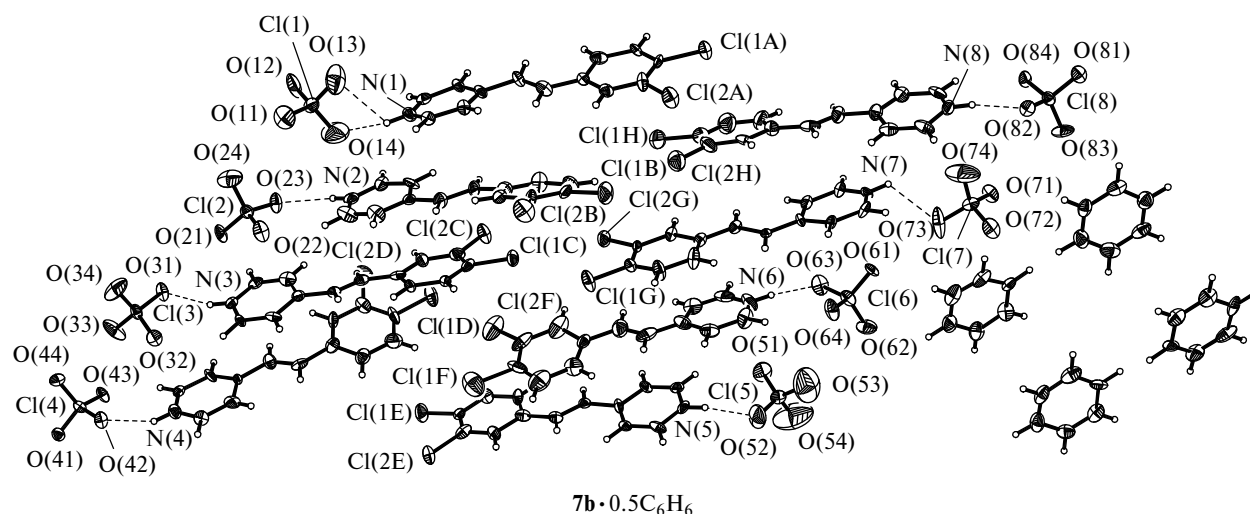


**Fig. 6.** Structures of the formula units in the crystal of **7b**·0.5C<sub>6</sub>H<sub>6</sub> (eight independent molecules of **7b**). The nonhydrogen atoms are shown as displacement ellipsoids at the 50% probability level. The hydrogen bonds are shown as dashed lines.

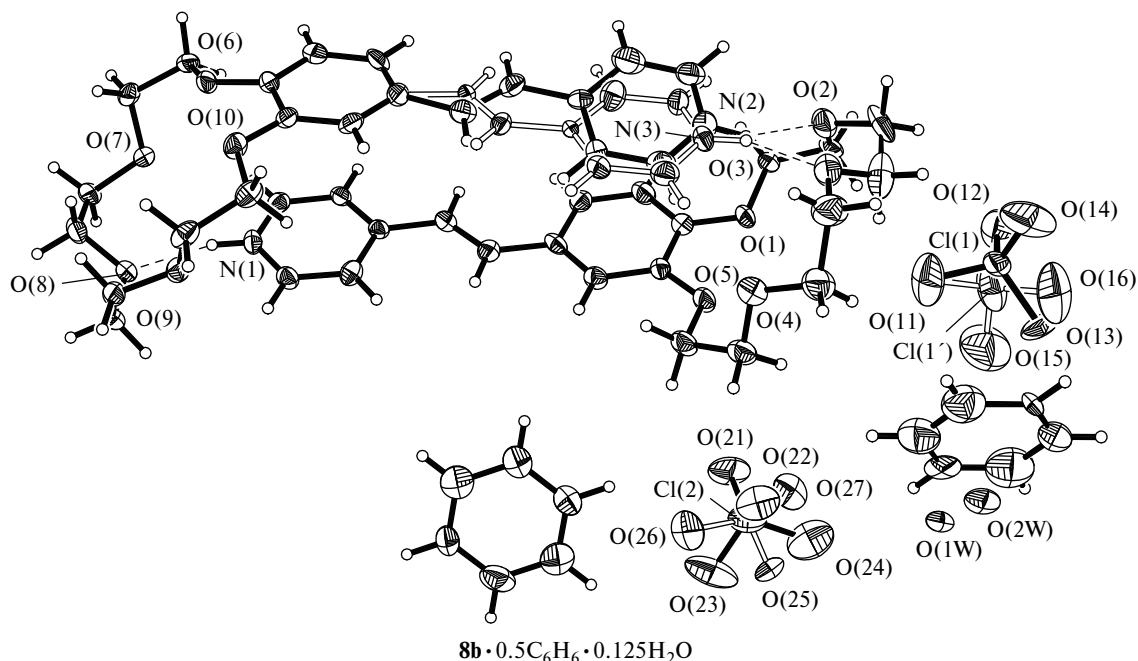


**Fig. 7.** Structures of the formula units in the crystal of  $8b \cdot 0.5C_6H_6 \cdot 0.125H_2O$  (two independent molecules of **8b**, one of them as two *s* conformers). The nonhydrogen atoms are shown as displacement ellipsoids at the 30% probability level. The hydrogen bonds are shown as dashed lines.

In the structure of  $9b \cdot NH_4ClO_4$ , the inorganic salt appears in the crystalline substance due, apparently, to the relatively fast hydrolysis of acetonitrile in the presence of an excess of perchloric acid. The  $NH_4^+$  ion is encapsulated in the cavity of the 18-crown-6 moiety and forms hydrogen bonds with the oxygen atoms. The lengths of the  $N(2)H \cdots O$  hydrogen bonds are in the range of 1.78–2.40 Å, and the angles at the H atoms are in the range of 130–162°. Two units of the macrocycle are disordered over two positions with the occupancy ratio of 0.63 : 0.37.

**Crystal packings of protonated styrylpyridines.** The projection of the crystal packing of **1b** along the *b* axis of the crystal is shown in Fig. 9, *a*. This compound has the packing motif *e* (see Fig. 1) similar to one of the three packings found<sup>23,24</sup> in the crystalline phases of related styryl dye **1a**. In the dimers, the molecules are related by centers of symmetry due to which they are arranged in a head-to-tail fashion. In the dimer, the conjugated systems are projected onto each other with the distances  $d_1$  (see Scheme 1) between the ethylene carbon atoms equal to 3.70 and 3.69 Å for the major and minor *s* conformers, respectively,

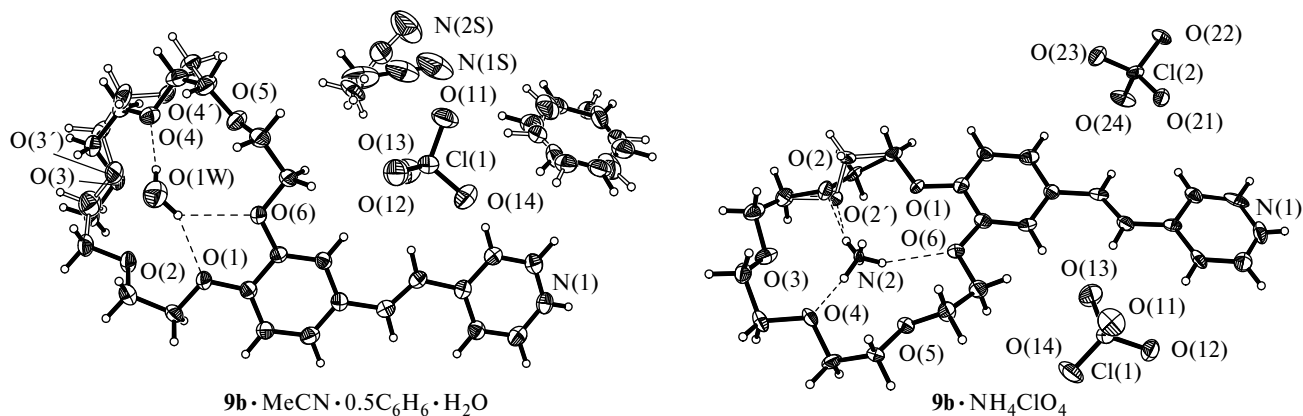


**Fig. 8.** Structures of the formula units in the crystals of  $9b \cdot MeCN \cdot 0.5C_6H_6 \cdot H_2O$  (the disordered moiety of the macrocycle and solvent molecules) and  $9b \cdot NH_4ClO_4$  (the disordered moiety of the macrocycle). The nonhydrogen atoms are shown as displacement ellipsoids at the 50% probability level. The hydrogen bonds are shown as dashed lines.

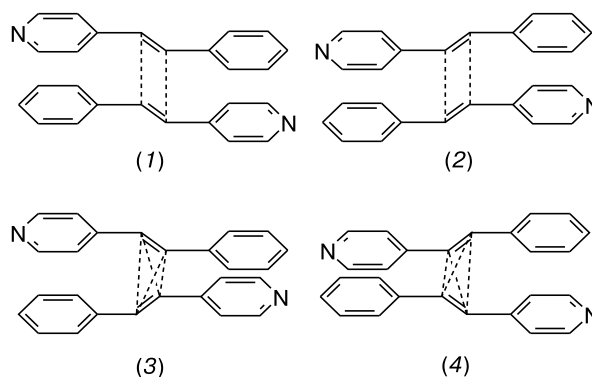


whereas the corresponding distances between the adjacent dimers,  $d_2$ , are 5.56 and 5.51 Å in the absence of the mutual overlap (Fig. 9, *b*). This geometry indicates that the PCA reaction can proceed in this crystal to form the centrosymmetric *rcit* isomer of the cyclobutane derivative, which correlates well with the relatively high rate of this reaction in a polycrystalline film of compound **1b** (see Table 1).

The repeated X-ray diffraction study of a single crystal irradiated with visible light for nine days was not performed because of a considerable loss in the quality of the crystal, which was covered with cracks, became turbid, and began to disintegrate. Evidently, the degradation of the single crystal is caused by the PCA reaction that proceeds in the single crystal. It is known<sup>20,22,24,25</sup> that the presence of a soft mobile shell around the dimer preorganized for the PCA reaction is essential for the single crystal to remain intact in the course of this reaction. In the case of styryl dyes **1a–9a**, this shell is created together by translationally and rotationally mobile perchlorate anions and solvent aromatic molecules, as well as by the conformationally flexible moieties of the dyes. In the crystals of **1b**, which contain no solvent molecules and conformationally flexible moieties, the dimers are surrounded only by  $\text{ClO}_4^-$  ions, whose mobility is apparently insufficient for the formation of a soft shell. In addition, in this case the shell created by the anions around the dimers has high rigidity due to the formation of hydrogen bonds between the anions and the  $\text{N}^+-\text{H}$  groups of the cations. The presence of these hydrogen bonds in the crystal results in the formation of tetramers consisting of two cations and two anions (see Fig. 9). The  $\text{O}\cdots\text{N}/\text{O}\cdots\text{H}$  distances between the cations and anions are 3.00/2.19, 3.15/2.53 and 2.88/2.03, 3.31/2.82 Å for the major and minor *s* conformers, respectively.

It should be noted that the dynamic process of the bicycle-pedal isomerization inevitably leads to a decrease

in the probability of the PCA reaction for the following reason. At each instant of time, four different mutual arrangements of the molecules in dimers can take place in the crystals.



Only two of these arrangements (1 and 2) meet the conditions necessary for the reaction to occur, because they contain antiparallel ethylene groups, whereas in the two other cases (3 and 4), these groups are in a staggered arrangement.

The crystal packing of protonated nitrostyrylpyridine **2b** is shown in two projections in Fig. 10. It is similar to the crystal packing of related styryl dye **2a**.<sup>23,24</sup> Both these structures consist of centrosymmetric stacks arranged in a *syn*-head-to-tail fashion.

In the crystal of **2b**, the stacks are composed of dimers with a short distance between the ethylene groups in the dimers (3.77 Å; in dye **2a**,  $d_1 = 3.71$  Å) and a substantially longer distance between the ethylene groups of the adjacent dimers in the stack (4.69 Å; in dye **2a**,  $d_2 = 4.59$  Å), which corresponds to the conditions of the PCA reaction. In the dye, this reaction proceeds in the light quite rapidly. The process became noticeable already after 30 min since the crystals were cracked and turned turbid, which was accompanied by the degradation of the single crystal. The

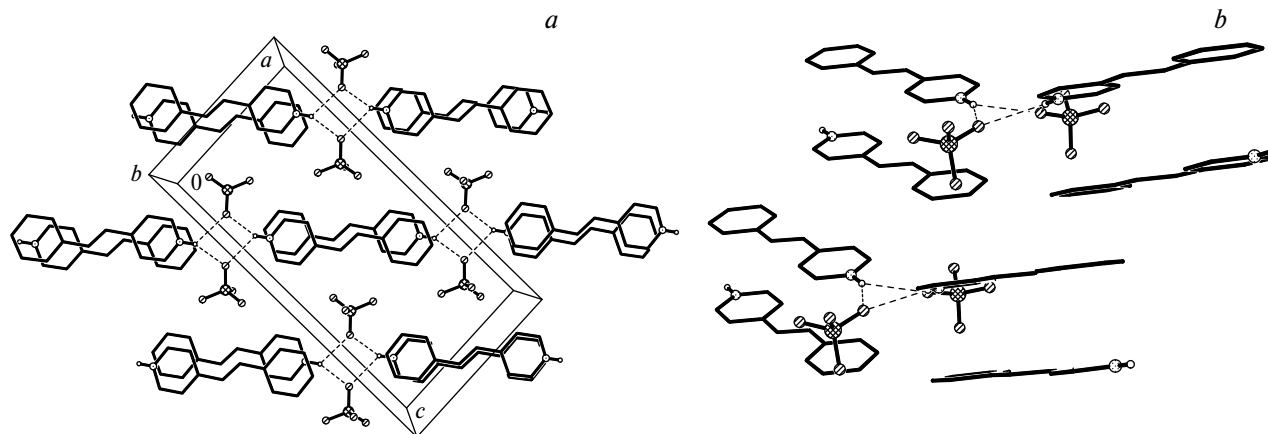


**Fig. 9.** Projections of the crystal packing of **1b** along the *b* axis (*a*) and a fragment of the sandwich-herringbone motif (*b*) in this packing. Only the major *s* conformers of **1b** are shown for simplicity. The hydrogen bonds are shown as dashed lines.

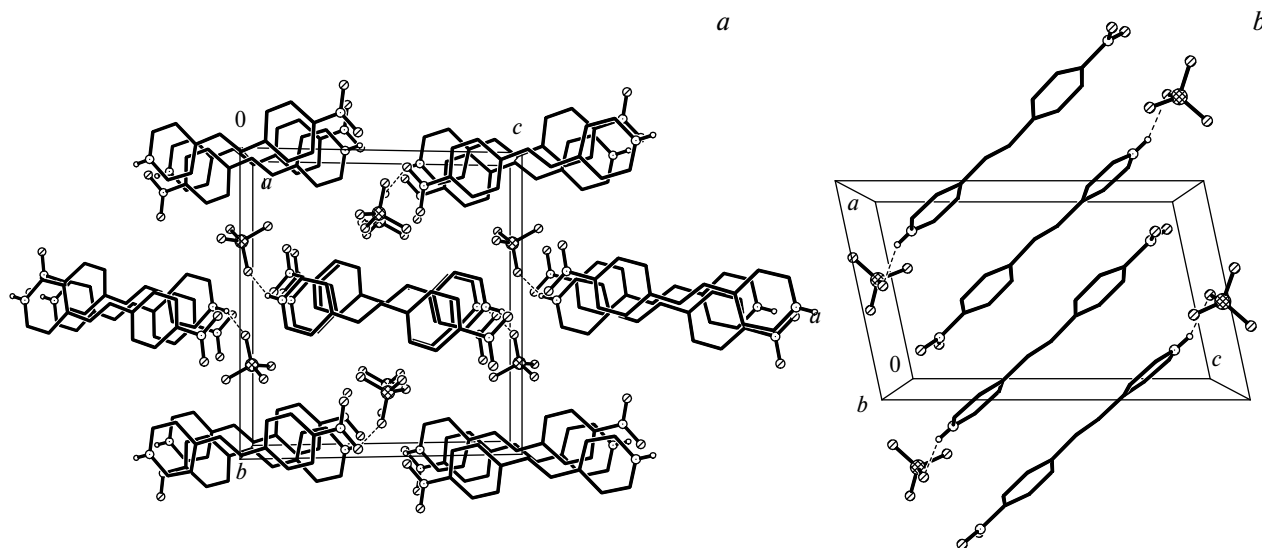


Fig. 10. Projections of the crystal packing of **2b** along the *a* (a) and *b* axes (b).

degradation of the single crystals of dye **2a** upon their irradiation occurs due to the absence of the soft mobile shell around the dimers, whose role is to provide the reduction of the steric strain in the crystal in the course of the PCA reaction. The crystals of **2b** exhibit high resistance to light and show no visual evidence of the degradation upon irradiation for one week, which correlates with the low rate of the photoreaction in a polycrystalline film of this compound (see Table 1). This is due to hydrogen bonds with the participation of the anions,  $N^+-H$ , and the nitro groups of the cations (Fig. 11).

The  $N^+-H$  group of the cation is involved simultaneously in two hydrogen bonds, viz., the bonds with the perchlorate oxygen atom (the  $N(1)...O(11)$  and  $H(1B)...O(11)$  distances are 2.86 and 2.11 Å, respectively) and the oxygen atom of the nitro group of the adjacent molecule (the  $N(1)...O(1A)$  and  $H(1B)...O(1A)$  distances are 3.03 and 2.59 Å, respectively). This hydrogen bond network results in a quite rigid framework preventing the atoms from shifting in the course of the PCA reaction in the crystal. However, at the ninth day of irradiation, first evidence of the crystal degradation, such as the surface

cracking and turbidity, were observed. In this step, the repeated single-crystal X-ray diffraction study was performed, which revealed the simultaneous presence of the starting compound **2b** and the centrosymmetric *rcft* isomer of cyclobutane **11** that was formed in the course of the PCA reaction (Fig. 12).

As expected, the PCA reaction proceeds in dimers with a relatively short distance between the ethylene groups and is accompanied by a decrease in the unit cell volume by 1%. The styrylpyridine/cyclobutane molar ratio in **2b/11** was 0.60 : 0.40 (the degree of conversion was 57%). The anion experiences strong rotational motion. The subsequent irradiation of the single crystal led to a considerable loss in its quality, which made it impossible to follow the accumulation of the photoreaction product. Therefore, in the case under consideration, the single crystal finally underwent degradation; however, due to the low rate of the PCA reaction, we succeeded in detecting the presence of the cyclobutane derivative by X-ray diffraction.

The crystals of **3b**·0.5C<sub>6</sub>H<sub>6</sub> (Fig. 13, a) are composed of translationally related stacks of cations arranged in a head-to-head fashion, the independent cations forming

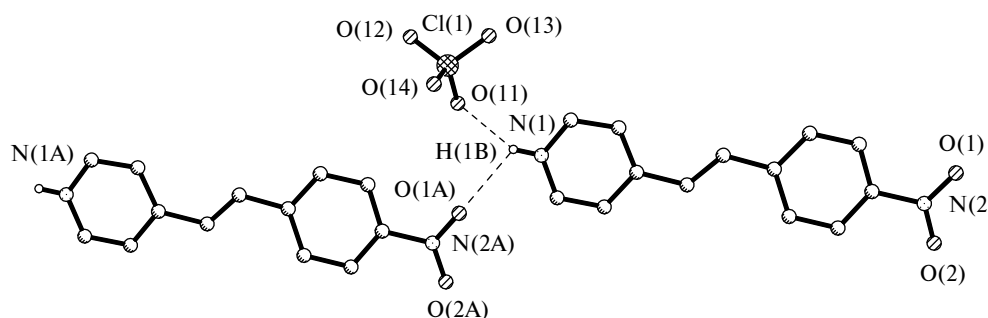
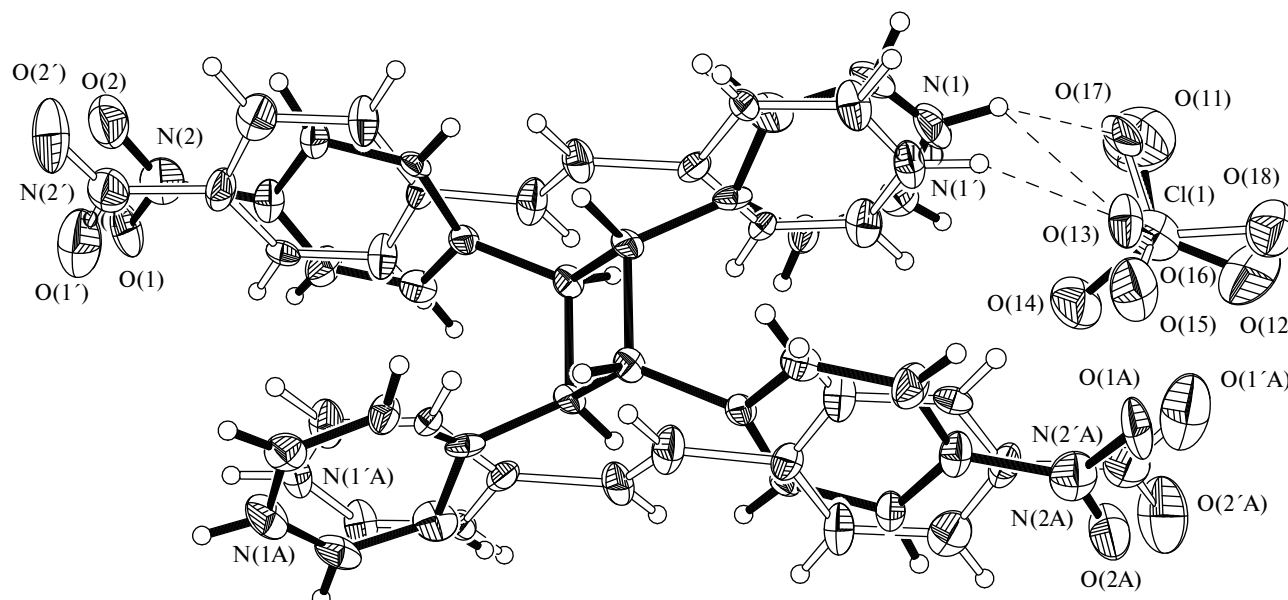


Fig. 11. Hydrogen bond network in the crystal structure of **2b**.



**Fig. 12.** Structural units in the crystal of **2b/11** (irradiation for 9 days) showing the simultaneous presence of the starting styrylpyridine and the *rac* isomer of cyclobutane. The atoms labeled with A are related to the unlabeled atoms by symmetry operations. The nonhydrogen atoms are shown as displacement ellipsoids at the 40% probability level. The hydrogen bonds are shown as dashed lines.

individual stacks. The disordered benzene solvent molecules are in the immediate vicinity of the stacks formed by the disordered cations, in which the bicycle-pedal isomerization can take place. Evidently, this is indicative of the dynamic character of the disorder of the solvent molecules. In addition, the disordered anions form hydrogen bonds with the  $N^+-H$  groups of the disordered cations, which is also indicative of the dynamic character of disorder of these structural units. Apparently, the whole sequence of dynamic processes has the common origin, *viz.*, the dynamic process of the bicycle-pedal isomerization.

In the crystals of **3b**·0.5C<sub>6</sub>H<sub>6</sub>, both perchlorate anions are involved in hydrogen bonds. The system of hydrogen bonds, by which the ordered cations and anions are linked to each other, is similar to that observed in the crystals of **1b** (Fig. 13, *b*). The O(11D)...N(1C) and O(11D)...H(11C) distances are 3.33 and 2.85 Å, respectively; the O(11C)...N(1C) and O(11C)...H(11C) distances are 2.90 and 2.10 Å, respectively. The disordered cations and anions are also linked together by hydrogen bonds to form tetramers. The O...N and O...H distances for two *s* conformers are in the ranges of 2.88–3.41 and 2.05–2.87 Å, respectively.

In this case, it is evident that the packing motif of protonated styrylpyridine **3b** is similar to that of related dye **3a**.<sup>23,24</sup> The head-to-head stacks found in **3b**·0.5C<sub>6</sub>H<sub>6</sub> are unpromising for the PCA reaction in the crystal. In these stacks, adjacent cations are strongly shifted with respect to each other (see Fig. 13, *b*), so that the distance between the adjacent ethylene groups is 6.87 Å. Earlier, it has been noted that the PCA reaction in compounds **3a,b**

is impossible because of the strong electron-donating properties of the NMe<sub>2</sub> substituent. Nevertheless, the structural studies of these compounds contribute to a deeper knowledge on the possible types of crystal packings. Therefore, the PCA reaction in the crystal of **3b**·0.5C<sub>6</sub>H<sub>6</sub> is impossible not only because of the chemical nature of the compound but also because of the formal crystallographic reasons.

Based on the fact that the crystal packings of protonated styrylpyridines **1b**–**3b** and related dyes **1a**–**3a** are pairwise similar, the same situation would be expected for compounds **4b** and **5b** containing the methoxy or methylsulfanyl group, respectively, in the benzene ring. Styryl dyes **4a** and **5a** crystallize in two pairs of isostructural crystal modifications.<sup>23,24</sup> One of these modifications consists of the centrosymmetrically related stacks formed by cations arranged in a head-to-tail fashion, whereas another modification is composed of translationally related head-to-head stacks. We succeeded in preparing two crystal modifications for both compounds **4b** and **5b**.

In the crystal packings of **4b** and **4b**·0.5C<sub>6</sub>H<sub>6</sub> (Fig. 14), there are translationally related stacks of cations. In the structure of **4b**·0.5C<sub>6</sub>H<sub>6</sub>, these stacks form layers alternating with layers formed by anions and benzene solvent molecules. The geometry of the hydrogen bond between the cations and anions is similar to that found in the structures of **1b** and **3b**·0.5C<sub>6</sub>H<sub>6</sub>; the corresponding O...N and O...H distances are in the ranges of 2.91–3.23 and 2.05–2.63 Å, respectively. The head-to-head packing motif, like that in the structure of **3b**·0.5C<sub>6</sub>H<sub>6</sub>, is associated with a substantial shift of the adjacent cations of **4b** in the stacks in parallel planes. In the crystals of **4b** and **4b**·0.5C<sub>6</sub>H<sub>6</sub>, the

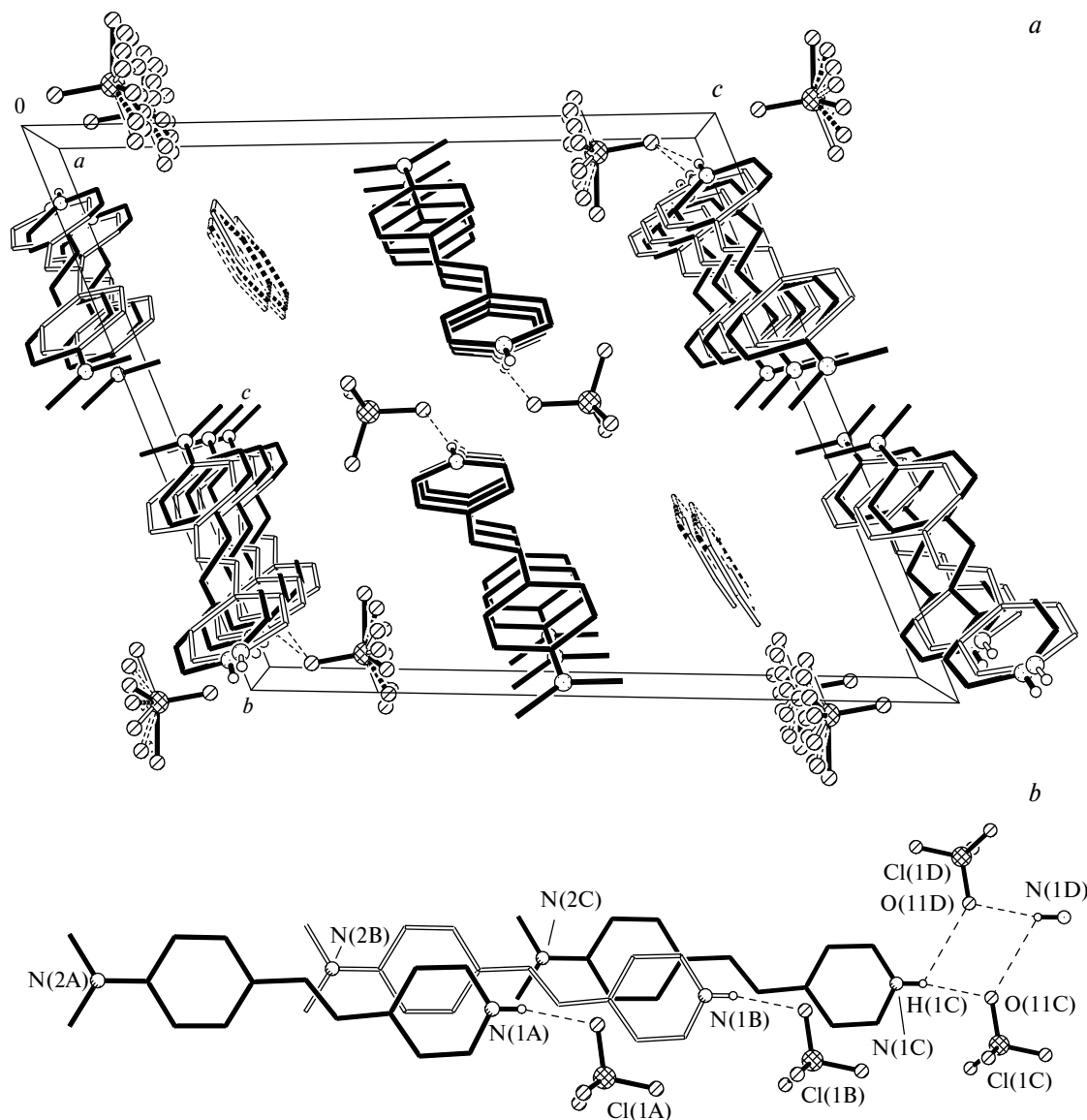


**Fig. 13.** Projection of the crystal packing of **3b** · 0.5C<sub>6</sub>H<sub>6</sub> along the *a* axis (*a*) and a fragment of the stack formed by the ordered cations projected onto the mean plane of the cation labeled with A (*b*). The hydrogen bonds are shown as dashed lines.

distances between the ethylene groups are 8.82 and 6.79 Å, respectively, which indicates that the solid-state PCA reaction cannot proceed. Evidently, similar types of the molecular packing take place in a polycrystalline film of compound **4b**, which accounts for the absence of the [2+2] cycloaddition products after the long-term irradiation (see Table 1).

The crystal packing of **5b** consists of centrosymmetrically related stacks extended along the *a* axis of the crystal, with cations being arranged in a *syn*-head-to-tail fashion (Fig. 15). These stacks are divided into dimers, like those in the crystal of **2b**. The distance  $d_1$  in the dimer is 3.79 Å, and the corresponding distance  $d_2$  between the adjacent dimers is 4.55 Å, *i.e.*, the conditions necessary for the solid-state PCA reaction are met.

This crystal also consists of tetramers formed by two cations and two anions linked together by hydrogen bonds (see Fig. 15). The O(11A)...N(1B), O(11A)...HN(1B) and O(11B)...N(1B), O(11B)...HN(1B) distances are 3.07, 2.24 and 3.04, 2.20 Å, respectively, and the angles at the H atoms are 134 and 136°.

Although the similar stacking motif is observed in the crystal packing of one modification of dye **5a**, the crystal packing of compound **5b** has substantial differences, among which the formation of secondary bonds between adjacent sulfur atoms is one of the most important feature.

The S...S distance is 3.386(5) Å, the S→S vector lies almost on the extension of one of the bonds formed by the sulfur atom, and the S...S—C<sub>Ar</sub> angle is 162.2(3)°. The observed geometry corresponds to the *n*-σ\* secondary bond

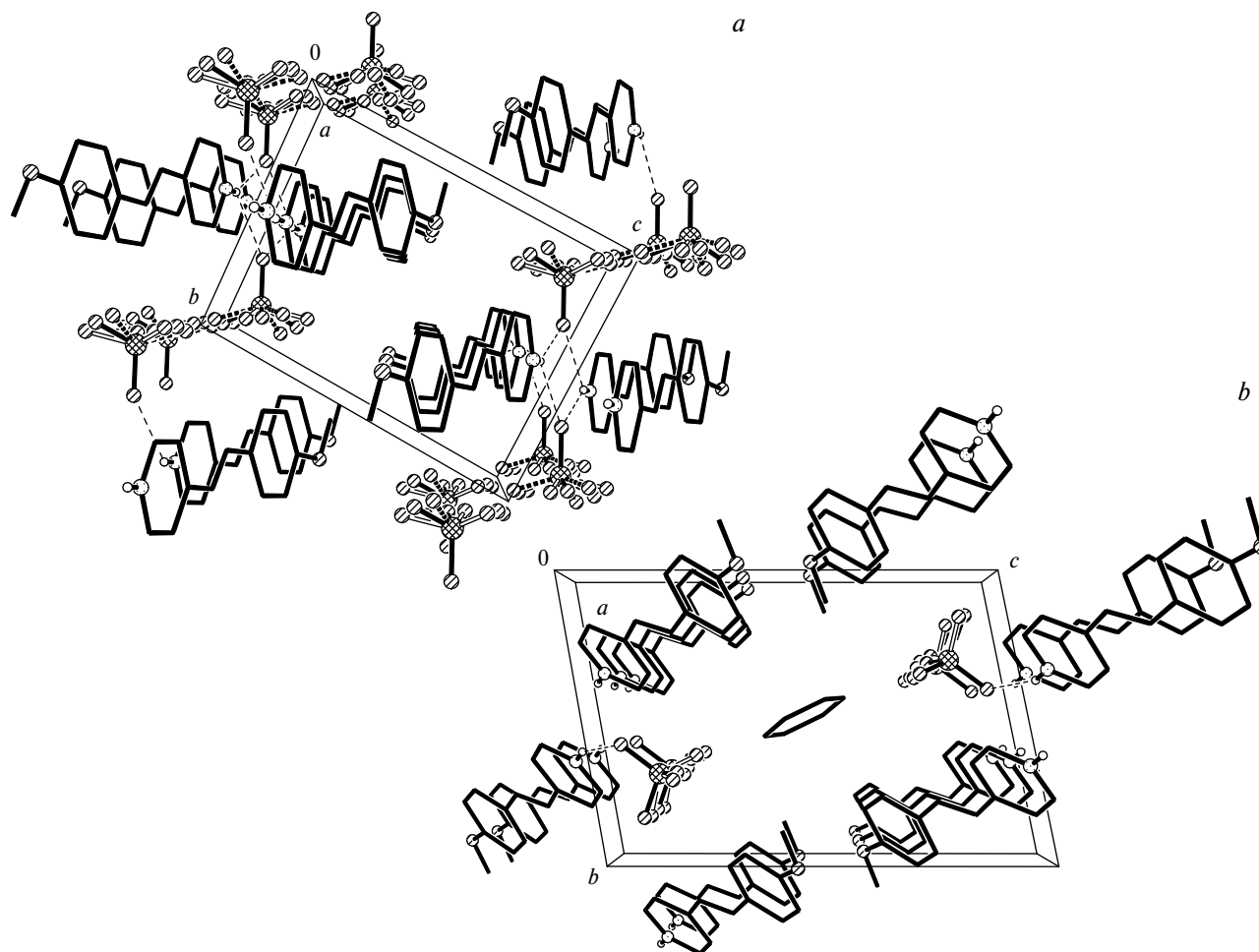


**Fig. 14.** Projections of the crystal packings of **4b** (a) and **4b**·0.5C<sub>6</sub>H<sub>6</sub> (b) along the *a* axis. Only the major *s* conformers of the cations in the structure of **4b**·0.5C<sub>6</sub>H<sub>6</sub> are shown for simplicity. The hydrogen bonds are shown as dashed lines.

with the participation of the unoccupied  $\sigma^*$  orbital of the S—C<sub>Ar</sub> bond of one sulfur atom and the lone pair at the  $sp^2$ -hybrid orbital of another sulfur atom. This type of interactions is often observed in organic compounds of divalent sulfur. We analyzed the intermolecular S...S contacts based on the data deposited in the Cambridge Crystallographic Data Centre (CCDC, version 5.30).<sup>43</sup> Figure 16 shows the histogram of these contacts. The shorter the  $d(\text{S}...\text{S})$  distance, the more pronounced the directionality of this interaction. At shorter  $d(\text{S}...\text{S})$  distances, the configuration of the bonds at the sulfur atom has a more pronounced T-shaped geometry. The distance determined in the present study is approximately in the middle of the range characteristic of S...S interactions.

Upon irradiation of crystals of compound **5b**, they remain intact during a certain period of time, but then they start to crack and undergo rapid degradation. Attempts to detect the intermediate formation of the photoproduct in the crystal by X-ray diffraction failed; however, according to the <sup>1</sup>H NMR spectroscopic data, the irradiation of

a polycrystalline film of compound **5b** leads to a relatively fast conversion into the corresponding *rect* isomer of cyclobutane (see above). This is indicative of the similar packing motif of **5b** in the film.

The crystal packing of **5b**·0.76C<sub>6</sub>H<sub>6</sub>·0.14H<sub>2</sub>O is also similar to one modification of dye **5a**. In the unit cell, all 11 independent molecules of protonated styrylpyridine form very loose and poorly ordered head-to-head stacks (see Fig. 4). In these stacks, the ethylene bonds of the adjacent molecules have both parallel and staggered mutual orientations. The distances between these molecules are 4.64–6.76 Å, which is unfavorable for the PCA reaction.

The crystal packing of **6b<sup>m</sup>** (Fig. 17, a) consists of alternating layers of anions and cations arranged both in a head-to-tail and head-to-head fashion. The aromatic moieties are stacked onto each other in three different ways: by pairs of dimethoxybenzene moieties, by pairs of pyridine moieties, and by a combination of dimethoxybenzene/pyridine moieties. The ethylene groups are not

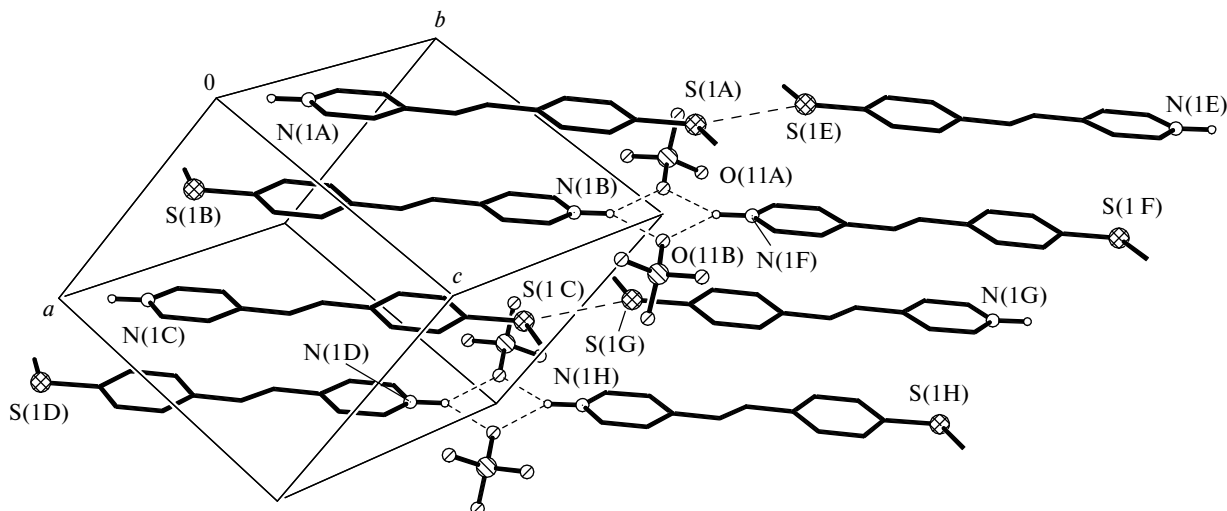


Fig. 15. The crystal packing of **5b**. The hydrogen bonds and the S...S contacts are shown as dashed lines.

involved in the  $\pi$ -overlap with each other; their mutual shift is 6.09–7.07 Å, which is unsuitable for the PCA reaction. The mutual arrangement of the cations in the layer apparently corresponds to the optimal set of weak interactions. These are, on the one hand, stacking interactions between the aromatic moieties and, on the other hand, hydrogen bonds. The major *s* conformer forms a  $N^+ - H \cdots O$  hydrogen bond with one of the methoxy groups of the adjacent cation related to the original cation by the *c*-axis translation. The  $N(1) \cdots O(2A)$  and  $H(1N) \cdots O(2A)$  distances are 2.98 and 2.11 Å, respectively; the angle at the  $H(1N)$  atom is 167°; these hydrogen bonds link the cations together to form chains running along the *c* axis (Fig. 17, *b*). The minor *s* conformer forms a weak hydro-

gen bond with the  $Cl(2)O_4^-$  anion. The  $N(1') \cdots O(21)$  and  $H(1'N) \cdots O(21)$  distances are 3.02 and 2.35 Å, respectively; the angle at the  $H(1'N)$  atom is 133°.

The crystals of **6b<sup>o</sup>** consist of translationally related stacks of cations arranged in a head-to-head fashion (Fig. 18). This packing is unsuitable for the PCA reaction, because the distance between the ethylene groups of adjacent cations is too large ( $\geq 4.99$  Å). Two symmetry-related perchlorate anions form the  $N^+ - H \cdots OClO_3$  hydrogen bonds with the cation; the  $N \cdots O$  and  $H \cdots O$  distances are 2.91 and 2.06 Å, respectively; the angle at the H atom is 162°.

The crystal packings of **6b<sup>m</sup>** and **6b<sup>o</sup>** have no analogies with the packing of related styryl dye **6a**, whose crystals are composed of centrosymmetrically related stacks of cations arranged in a head-to-tail fashion.<sup>23,24</sup> This has a crucial effect on the ability of compounds **6a** and **6b** to undergo the solid-state PCA reaction. In the case of a polycrystalline film of dye **6a**, the phototransformation proceeds rapidly and quantitatively to form the *rect* isomer of the cyclobutane derivative, whereas a film of compound **6b** proved to be insensitive to light (see Table 1).

Compound **7b** crystallizes as a benzene solvate (**7b**·0.5C<sub>6</sub>H<sub>6</sub>) with eight crystallographically independent formula units. In the crystal, independent cations are arranged in two types of low-symmetry head-to-head stacks (see Fig. 6) similar to those found in the crystals of **3b**·0.5C<sub>6</sub>H<sub>6</sub>, **4b**·0.5C<sub>6</sub>H<sub>6</sub>, **5b**·0.76C<sub>6</sub>H<sub>6</sub>·0.14H<sub>2</sub>O, and **6b<sup>o</sup>**. The distances between the atoms of the ethylene groups of adjacent cations are very large (4.63–6.54 Å), which excludes the PCA reaction in these crystals and accounts for their resistance to light. The hydrogen bond network in the crystal of **7b**·0.5C<sub>6</sub>H<sub>6</sub> with the participation of the  $N^+ - H$  groups and  $ClO_4^-$  ions is similar to the above-considered cases: the cations are involved in single and bifurcated hydrogen bonds with either one or two anions.

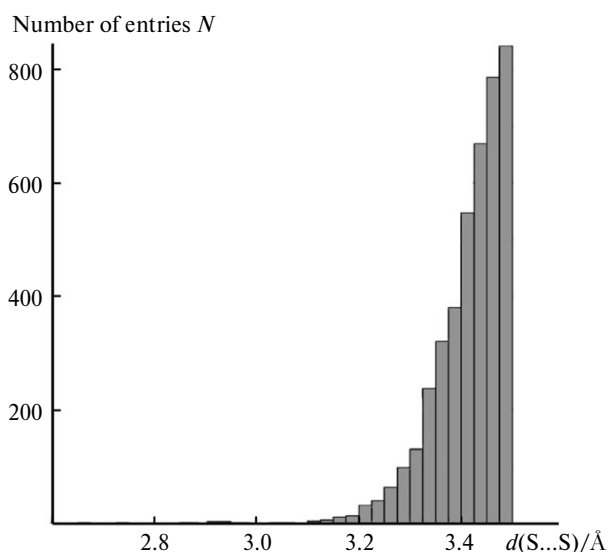
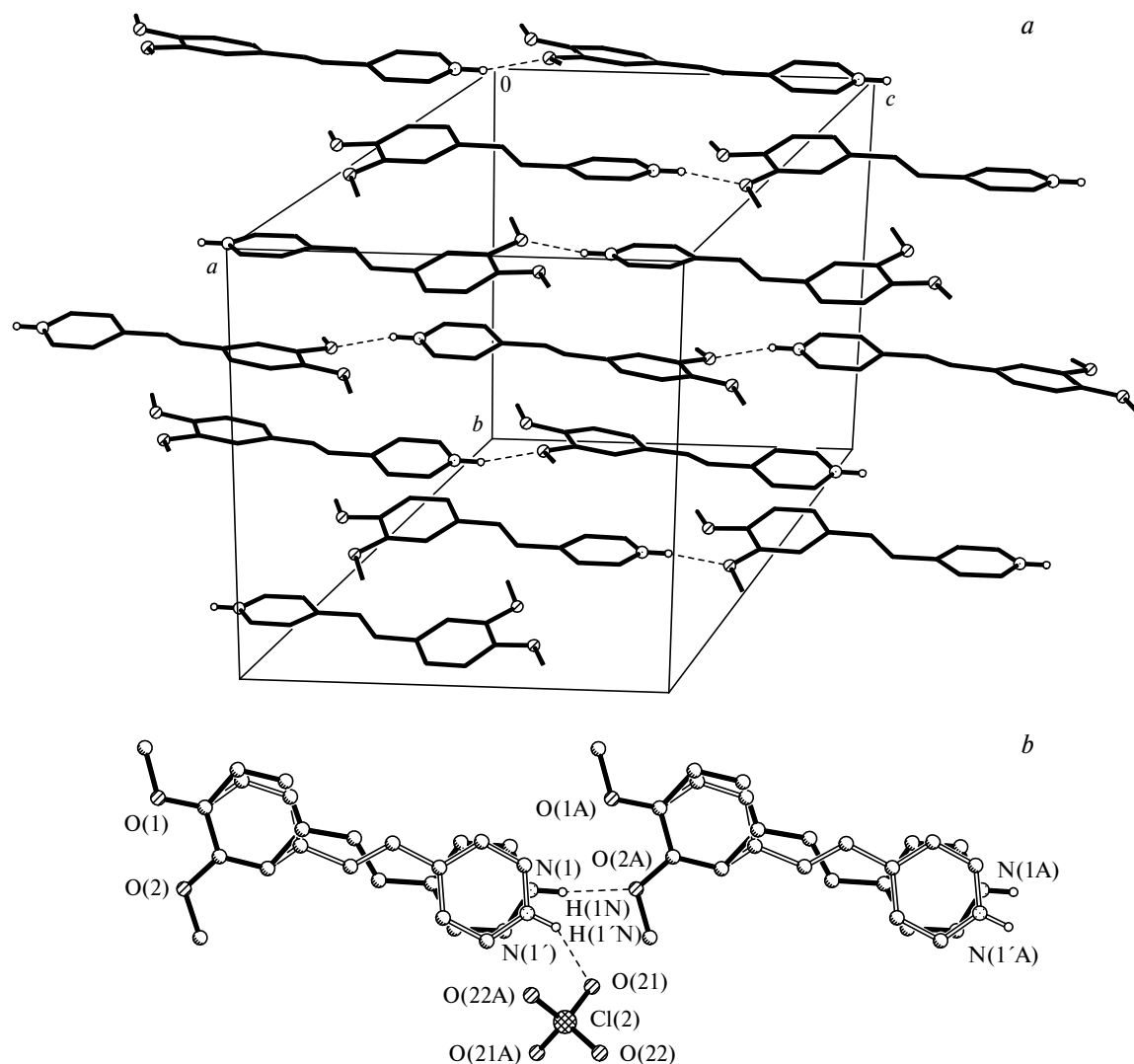


Fig. 16. Histogram of S...S contacts in organic sulfur(II) compounds extracted from the CCDC.



**Fig. 17.** One layer of the cations in the crystal packing of **6b<sup>m</sup>** (*a*, only the major *s* conformers are shown) and the hydrogen bond network (*b*). The hydrogen bonds are shown as dashed lines.

The long-term irradiation of a polycrystalline film of compound **7b** led to a very slow accumulation of two isomers of the cyclobutane derivative (see Table 1), which indicates that the translation motif prevails in the molecular packing of this compound. In the crystals of dye **7a** related to this styrylpyridine, the cations are arranged in a head-to-tail fashion to form centrosymmetric stacks.<sup>24</sup> In these crystals, the solid-state PCA reaction shows the same stereoselectivity but proceeds much more rapidly and is accompanied by the single-crystal degradation.

The crystal packing of compound **8b** is shown in Fig. 19. The presence of the 15-crown-5 ether moiety in the styrylpyridine molecule leads to the formation of dimers, in which the cations are linked together by single or bifurcated  $N^+H\cdots O(\text{macrocycle})$  hydrogen bonds. This is possible due to the conformational flexibility of the polyether ring allowing the ring to be bent in such a way that

the oxygen atom of the macrocycle most distant from the benzene ring is in close proximity to the  $N^+H$  group of the second molecule of the dimer. The hydrogen bonds (see Fig. 19, *b*) have the following parameters:  $N(1B)H\cdots O(8B)$ ,  $N(2B)H\cdots O(2B)$ ,  $N(2B)H\cdots O(3B)$ , and  $N(3B)H\cdots O(3B)$ , 1.92, 2.18, 2.15, and 1.90 Å, respectively; the angles at the H atoms are 167, 131, 149, and 156°.

The dimers are arranged in stacks along the *c* axis of the crystal. These stacks form layers, in which the contacts between adjacent stacks occur *via* the crown ether moieties. These layers are separated from each other by loose interlayers formed by the disordered anions and solvent molecules (see Fig. 19, *a*). The high degree of disorder of most of the components in the unit cell leads to a substantial loss of the quality of the crystal of **8b**·0.5C<sub>6</sub>H<sub>6</sub>·0.125H<sub>2</sub>O. However, this results in the higher stability of the crystal in the course of the possible PCA

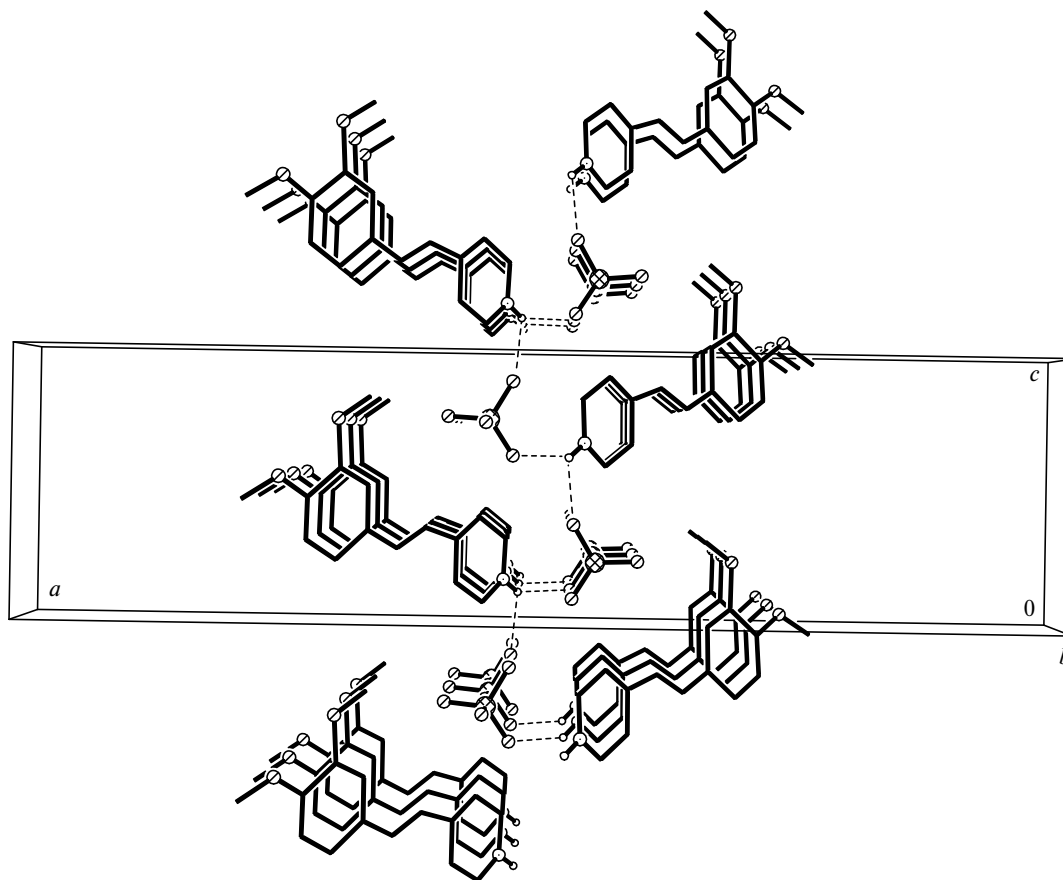


Fig. 18. Projection of the crystal packing of **6b**<sup>°</sup> along the *b* axis. The hydrogen bonds are shown as dashed lines.

reaction, because such a loose shell around the dimer pairs can reduce internal strains resulting from displacements of atoms in going from the dimeric structure to cyclobutane. It should be noted that the packing motif in this crystal is similar to that in the crystals of dye **9a**, where we have observed<sup>20</sup> the PCA reaction without single-crystal degradation.

Since each dimer consists of the ordered and disordered independent cations of **8b**, the ethylene bonds in these pairs are located one above another either in a staggered or almost antiparallel fashion (the twisting angle is only 17°). The latter mode of the mutual arrangement of the molecules meets the conditions of the solid-state PCA reaction, because the distances  $d_1$  are in the range of 3.45–3.62 Å. This is why the crystal was subjected to long-term irradiation, which was interrupted each second day for a short period of time to check the unit cell parameters, whose change would be indicative of the PCA reaction. However, the visual evidence of the impairment of the quality of the single crystal, such as the loss of the color, the opacity, and the surface cracking, as well as a slight change in the unit cell parameters, appeared only at the 11th day of irradiation of the single crystal. The X-ray diffraction study revealed the formation of the cyclo-

butane derivative along with the existence of the starting styrylpyridine in one and the same crystal of (**8b/13**)·C<sub>6</sub>H<sub>6</sub>·0.25H<sub>2</sub>O. The reflectivity of the single crystal noticeably deteriorated due to the appearance of numerous disordering elements. Figure 20 shows the main unit cell components of the irradiated crystal. It can be seen that the *rect* isomer of cyclobutane is produced by the cycloaddition of cations of **8b** in *syn* orientations. The occupancy ratio of two positions for the *s* conformers of the disordered cation (0.60 : 0.40) changes only slightly compared with the starting crystal, whereas the styrylpyridine/cyclobutane molar ratio is 0.73 : 0.27 (the degree of conversion is 42%). This fact confirms the dynamic character of the disorder with the result that the fraction of the minor *s* conformer of the starting compound consumed in the course of the PCA reaction is constantly replenished due to the bicycle-pedal isomerization. Once the PCA reaction partially proceeded, the unit cell volume decreased by only 0.5% compared with the initial value, although certain unit cell parameters substantially changed.

It is noteworthy that the further irradiation of the single crystal of (**8b/13**)·C<sub>6</sub>H<sub>6</sub>·0.25H<sub>2</sub>O during a few hours (the repeated experiment was performed 20 h after the beginning of the further irradiation of the crystal of



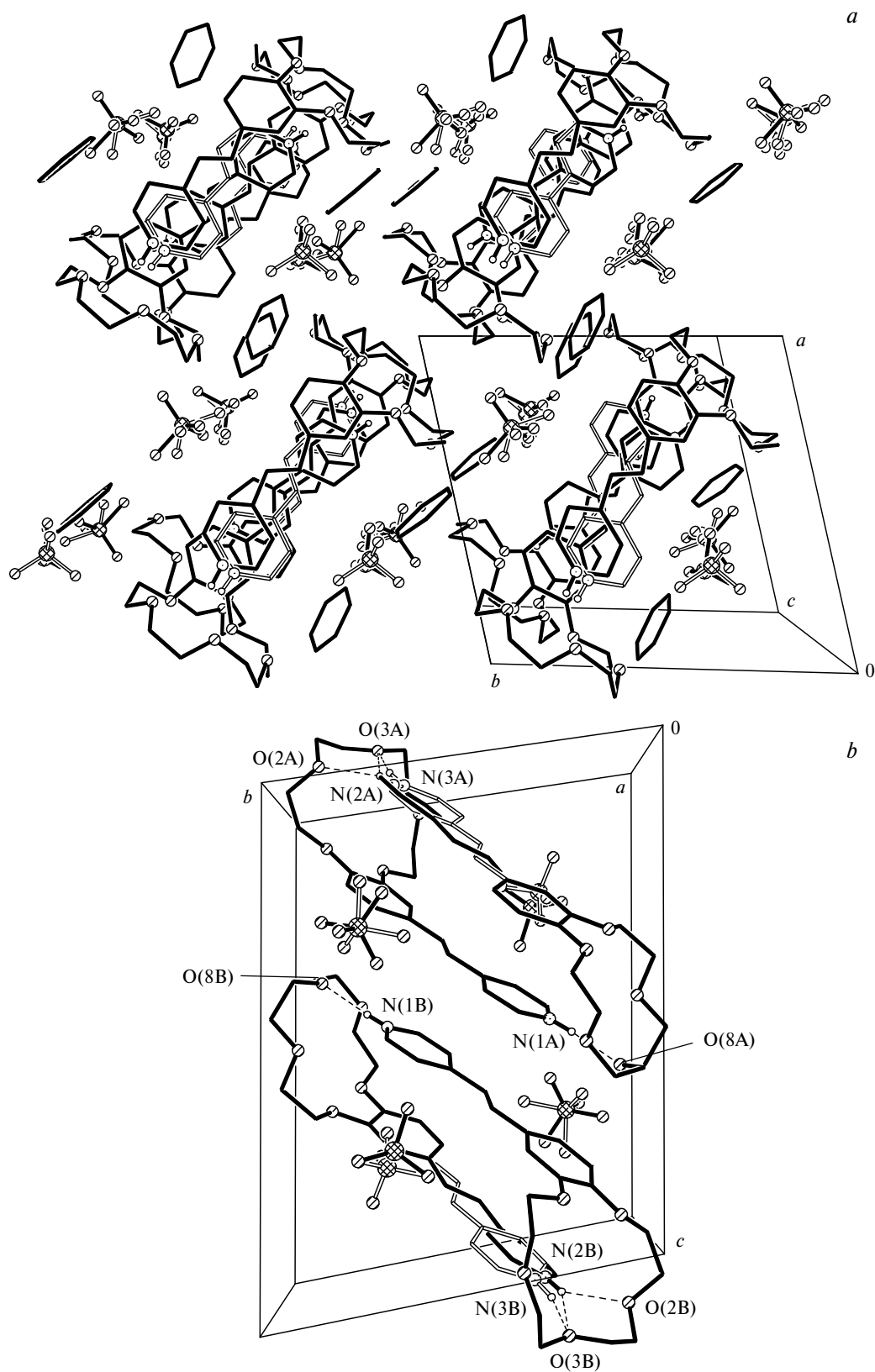


**Fig. 19.** Projections of the crystal packing of  $8b \cdot 0.5C_6H_6 \cdot 0.125H_2O$  along the  $c$  (a) and  $a$  axes (b). The hydrogen bonds are shown as dashed lines.

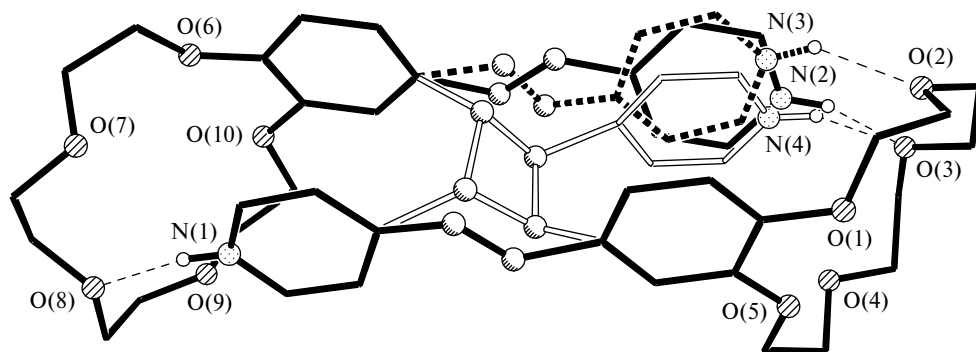


Fig. 20. Structures of the main components in the crystal structure of  $(8b/13) \cdot C_6H_6 \cdot 0.25H_2O$  (irradiation for 11 days) showing the simultaneous presence of the starting styrylpyridine and the *rcft* isomer of cyclobutane. The hydrogen bonds are shown as dashed lines.

$(8b/13) \cdot C_6H_6 \cdot 0.25H_2O$ ) led to the complete transformation of the starting compound into the corresponding *rcft* isomer of cyclobutane derivative  $13 \cdot C_6H_6 \cdot 0.25H_2O$ . A deep crack that formed in the single crystal resulted in the partial loss of its volume during the mounting of the crystal in a diffractometer. The processing of the experimental data gave the best result for the doubled unit cell compared to the starting crystal, which is indicative of the lowering of the symmetry. This is manifested in the disappearance of the centers of symmetry that relate the cations

in the stacks. Thus, the cations in the stacks are related not strictly by a center of symmetry but by a pseudo-center of symmetry resulting in the presence of two crystallographically independent stacks. Figure 21 shows the structure of  $13 \cdot C_6H_6 \cdot 0.25H_2O$ .

Each stack consists of unsymmetrical *rcft*-cyclobutane molecules. The conformations of the independent cyclobutanes are substantially different, particularly, in the region of the crown ether moieties, one of which is disordered, and the pyridine moieties (Fig. 22). The latter form

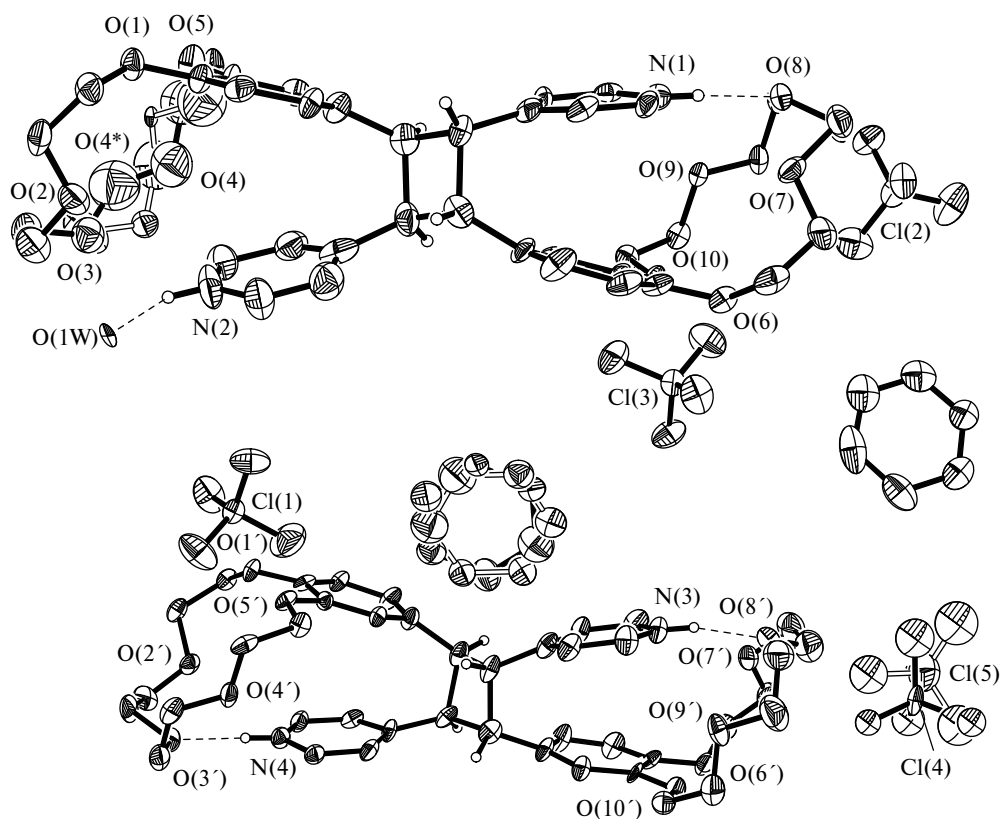


Fig. 21. Structure of  $13 \cdot C_6H_6 \cdot 0.25H_2O$  (irradiation for 12 days). The nonhydrogen atoms are shown as displacement ellipsoids at the 30% probability level. Most of the hydrogen atoms are not shown. The hydrogen bonds are shown as dashed lines.

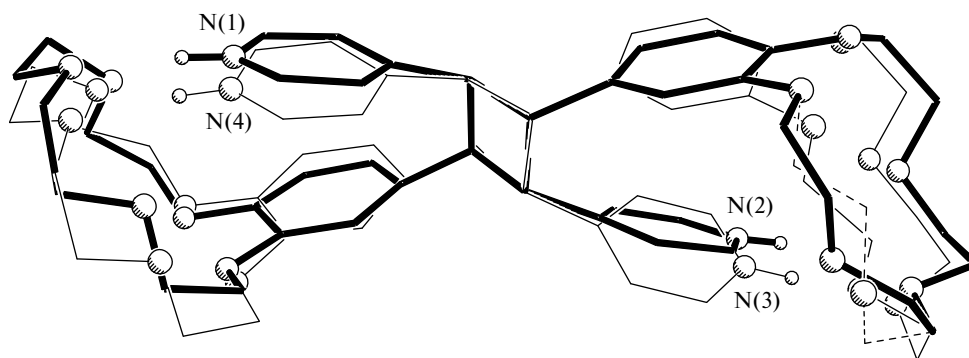


Fig. 22. Superposition of the independent cyclobutane dications in the structure of **13**·C<sub>6</sub>H<sub>6</sub>·0.25H<sub>2</sub>O using the cyclobutane rings and the nearest carbon atoms.

hydrogen bonds with either one of the oxygen atoms of the macrocycle or with the water solvent molecule (N<sup>+</sup>(1)H...O(8), N<sup>+</sup>(2)H...O(1W), N<sup>+</sup>(3)H...O(8'), and N<sup>+</sup>(4)H...O(3'), 1.88, 2.04, 1.90, and 1.88 Å, respectively, the angles at the H atoms are 176, 140, 163, and 173°, respectively).

The independent cyclobutanes are *rc*tt isomers, and their four-membered rings are nonplanar: the torsion angles in the rings vary from  $-4$  to  $5^\circ$  and from  $-15$  to  $14^\circ$  in two independent dications. This distinguishes cyclobutanes **13** from the earlier studied<sup>20–22,24,25,44</sup> centrosymmetric *rc*tt isomers of cyclobutanes, which have been synthesized by PCA in solution and crystals of styryl dyes and neutral 4-styrylquinoline, where the cyclobutane rings are ideally planar.

Apparently, due to the lowering of the overall crystal symmetry, the new structure is better adapted to the requirements of the crystal packing. The volume of the new unit cell is only 0.8% smaller than the doubled volume of the initial unit cell. The steric strains are partially reduced due to the more ordered positions of the perchlorate anions and solvent molecules. Evidently, the volume of the free space occupied by these small species decreases,

resulting in their fixation in particular positions with respect to other components of the unit cell.

The crystal packing of **9b**·MeCN·0.5C<sub>6</sub>H<sub>6</sub>·H<sub>2</sub>O is similar to that of the above-considered structure of **8b**·0.5C<sub>6</sub>H<sub>6</sub>·0.125H<sub>2</sub>O. The cations of compound **9b** form stacks composed of centrosymmetric head-to-tail dimers related to each other by centers of symmetry. The structure of the dimer formed *via* N<sup>+</sup>—H...O(macrocyclic) hydrogen bonds is shown in Fig. 23 (N(1)H...O(3A) and N(1)H...O(3'A), 2.01 and 2.14 Å, respectively; the angles at the H atoms are 155 and 170°). The ethylene bonds in the dimers and between the dimers are strictly antiparallel. The distance  $d_1$  in the dimers is 4.07 Å, and the distance between the ethylene groups of adjacent dimers in the stack,  $d_2$ , is even shorter (3.81 Å). Both distances are favorable for the PCA reaction giving the centrosymmetric *rc*tt isomer of cyclobutane. However, the formation of cyclobutane between the adjacent dimers should be accompanied by the decomposition of the dimer and a deeper conformational rearrangement of the cations. The process occurring simultaneously at the contacts  $d_1$  and  $d_2$  should be inevitably accompanied by the single-crystal degradation. The irradiation of the crystal led to its degradation.

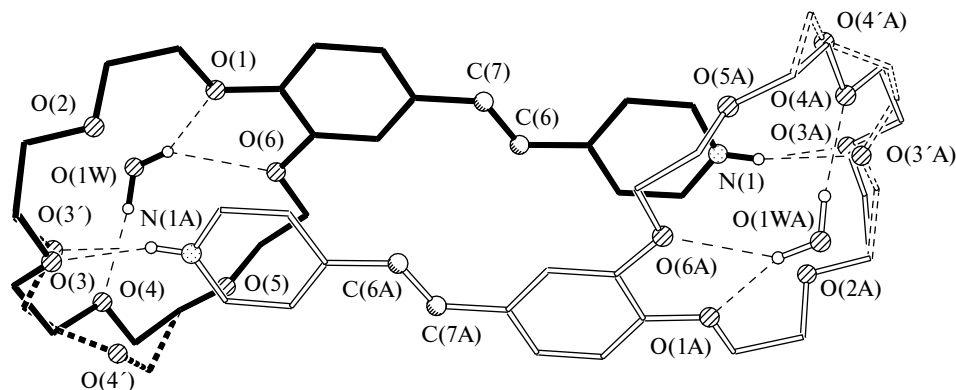


Fig. 23. Structure of the dimer pair in the crystal structure of **9b**·MeCN·0.5C<sub>6</sub>H<sub>6</sub>·H<sub>2</sub>O. The atoms labeled with A are related to the unlabeled atoms by symmetry operations. The hydrogen bonds are shown as dashed lines.

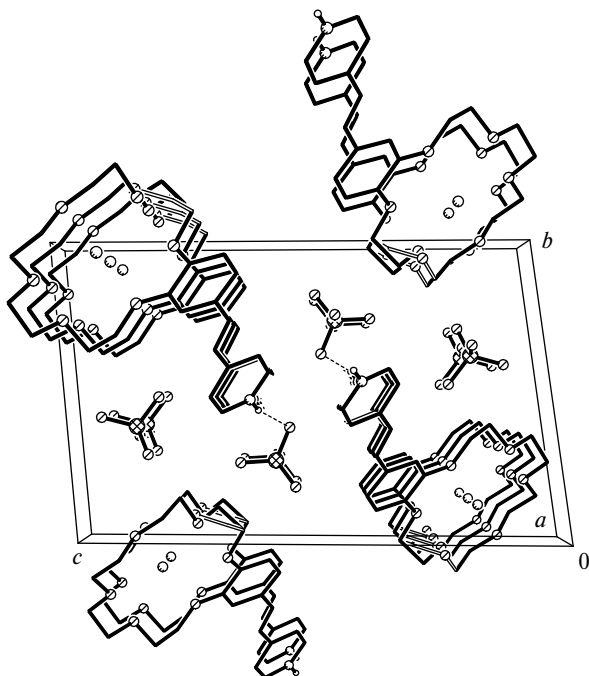


Fig. 24. Projection of the crystal packing of **9b** •  $\text{NH}_4\text{ClO}_4$  along the *a* axis. The hydrogen bonds are indicated by dashed lines.

The characteristic features of the crystal packing correlate well with the fast photoreaction in a polycrystalline film of compound **9b** and its stereochemical result according to the  $^1\text{H}$  NMR spectroscopic data.

In the crystal of related styryl dye **9a**, the molecular cations encapsulating a water molecule in the crown ether cavity are also arranged in centrosymmetric stacks in a *syn*-head-to-tail fashion, and the PCA reaction proceeds in these stacks to form the corresponding *rect* isomer of cyclobutane with the single crystal remaining intact.<sup>20</sup>

In the crystals of **9b** •  $\text{NH}_4\text{ClO}_4$  (Fig. 24), the organic cations form stacks, which are surrounded by rotationally mobile perchlorate anions and the crown ether moieties of adjacent stacks. The ammonium cation encapsulated in the cavity of the macrocycle forms a  $\text{N}^+ - \text{H} \cdots \text{OClO}_3$  hydrogen bond also with the perchlorate anion ( $\text{N} \cdots \text{O}$  and  $\text{H} \cdots \text{O}$ , 2.90 and 2.18 Å, respectively; the angle at the H atom is 165°). The stacks are arranged in a head-to-head fashion with a substantial shift of the ethylene groups in parallel planes ( $d = 6.23$  Å), due to which the PCA reaction cannot take place in this crystal packing.

The structure of the *rect* isomer of cyclobutane derivative **14** produced upon irradiation of a film of compound **9b** was confirmed by X-ray diffraction. For this purpose, a sample of compound **9b** irradiated in the solid phase was crystallized with the addition of 70%  $\text{HClO}_4$ . Cyclobutane **14** was studied by single-crystal X-ray diffraction. The structural units are shown in Fig. 25.

In the structure of **14** •  $\text{NH}_4\text{ClO}_4 \cdot \text{H}_2\text{O}$ , the position of one of the two independent perchlorate anions is fixed, whereas another anion is rotationally disordered over three positions (the occupancy ratio is 0.45 : 0.35 : 0.20). The  $\text{Cl}(1)\text{O}_4^-$  anion is involved in the hydrogen bond with the pyridinium moiety  $\text{C}_5\text{H}_4\text{N}(1)^+\text{H}$  or  $\text{C}_5\text{H}_4\text{N}(2)^+\text{H}$ : the

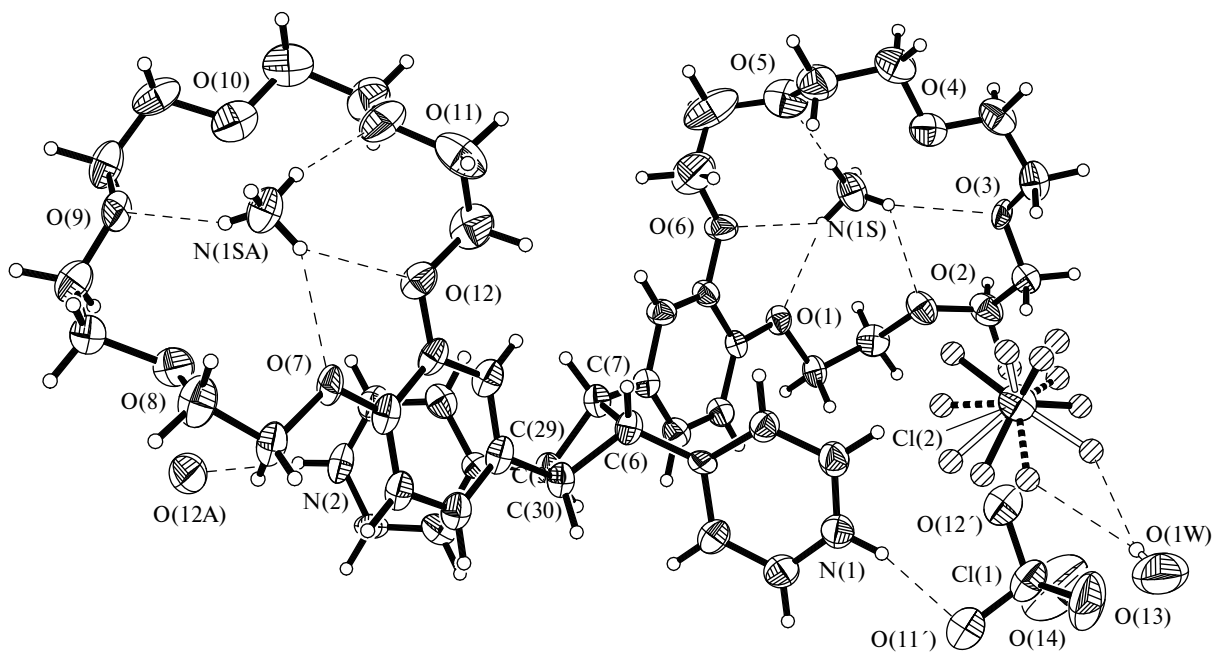


Fig. 25. Structure of **14** •  $\text{NH}_4\text{ClO}_4 \cdot \text{H}_2\text{O}$ . The nonhydrogen atoms are shown as displacement ellipsoids at the 50% probability level. The  $\text{N}(1\text{SA})^+\text{H}_4$  ion and the  $\text{O}(12\text{A})$  atom of the perchlorate anion are generated by symmetry operations. The hydrogen bonds are shown as dashed lines.

N(1)...O(11'), N(1)H...O(11') and N(2)...O(12A), N(2)H...O(12A) distances are 2.86, 2.00 and 2.91, 2.11 Å; the angles at the hydrogen atoms are 164 and 152°. In the crystal, the water molecule H<sub>2</sub>O(1W) forms hydrogen bonds with the oxygen atoms of the disordered anion Cl(2)O<sub>4</sub><sup>-</sup> (O(1W)H...O, 2.19 and 2.25 Å). The cavities of both crown ether moieties are occupied by ammonium ions, which appeared in the course of crystallization due to the hydrolysis of acetonitrile. The N—H...O hydrogen bonds have the following parameters: the distances vary from 1.94 to 2.45 Å and the angles at the H atoms are in the range of 126–178°.

It is interesting that the *rect* isomer of cyclobutane **14** characterized by a centrosymmetric bonding scheme occupies a general position in the crystal, and its cyclobutane ring adopts a nonplanar conformation, like in the crystal of **13**·C<sub>6</sub>H<sub>6</sub>·0.25H<sub>2</sub>O (the torsion angles in the ring C(6)—C(7)—C(29)—C(30) vary from -18 to 18°). In the centrosymmetric monoclinic unit cell (space group *P2/c*), the dication lies on a twofold axis with half occupancy. This cyclobutane is transformed into another isomer occupying virtually the same position in the unit cell by a twofold axis. The resulting pattern consists of two disordered equally occupied orientations of the dication (Fig. 26). Probably, this single crystal is a twin, with each component having lower symmetry (*Pc*). However, the lowering of the crystal symmetry by going to the space group *Pc* leads to the same result, *viz.*, the same disorder of the molecule. An examination of the doubling of the unit cell showed that it is impossible to go to the larger unit cell. At the same time, it cannot be ruled out that the observed type of disorder does occur in the crystal since, as can be seen from Fig. 26, the disorder elements have an almost single contour. It should be noted that these X-ray diffraction data are characterized by high accuracy, which allowed us to locate the hydrogen atoms of the cyclobutane corresponding to different disorder elements.

Therefore, the study of the characteristic features of the crystal packings of protonated 4-styrylpyridines showed that their crystals, as expected, consist primarily of stacks similar to the structures of related 4-styrylpyridine dyes. Many of them, particularly centrosymmetrically related stacks, are favorable for the solid-state PCA reaction. However, the translationally related stacks, which are unfavorable for the PCA reaction in the crystals, are equally often observed. This distinguishes protonated styrylpyridines from both neutral styrylpyridines, for which ladder packings without stacking interactions are most typical in the crystals, and the corresponding dyes, whose crystals are, as a rule, composed of centrosymmetrically related stacks formed by molecules arranged in a *syn*-head-to-tail fashion. This difference in the packing motifs of these compounds is attributed to the formation of hydrogen bonds between the N<sup>+</sup>—H group of the molecular cation and the perchlorate anion. The presence of hydrogen bonds in the crystal packing also leads to the higher overall rigidity of the structure and results in a decrease in the rate of the PCA reaction. Not only hydrogen bonds but also other weak directional interactions, for example, the S...S interaction, which is not observed in crystals of styryl dyes, can also play the structure-stabilizing function.

In spite of the above-mentioned increase in the rigidity of the structures, the photoreaction takes place both in single crystals and polycrystalline films of almost all the crystals under examination, which consist of centrosymmetrically related stacks composed of superimposed stacked dimers preorganized for the PCA reaction. In single crystals of protonated styrylpyridines, these reactions more often lead to their degradation than the corresponding reactions of related dyes.

In the single crystals of protonated 15-crown-5-containing styrylpyridine, which are stabilized not by hydrogen bonds between the cations and anions but by the N<sup>+</sup>—H...O(macrocyclic) hydrogen bonds linking the cat-

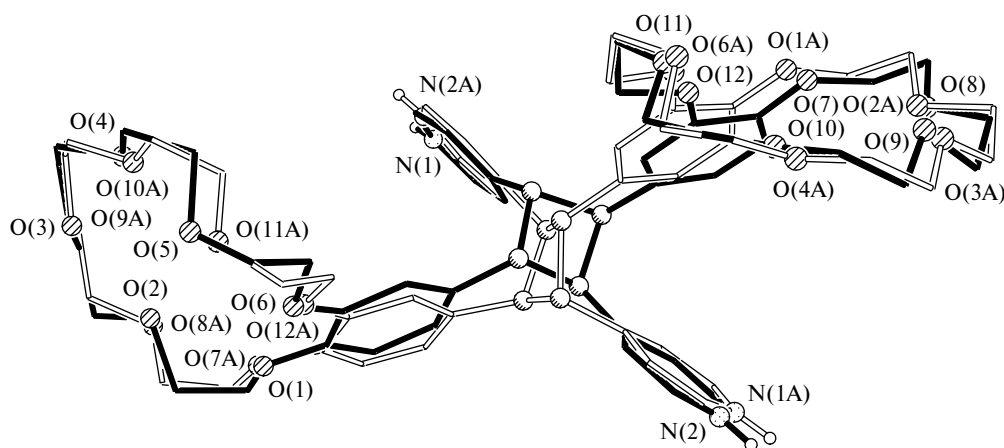


**Fig. 26.** Disorder of the cyclobutane dication in the crystal structure of **14**·NH<sub>4</sub>ClO<sub>4</sub>·H<sub>2</sub>O. The atoms labeled with A are related to the unlabeled atoms by symmetry operations.

ions to form hydrogen-bonded dimers, the PCA reaction was observed to proceed as the single-crystal-to-single-crystal reaction.

Only rotationally and translationally mobile anions, which are not fixed by hydrogen bonds, combined with solvent molecules, as well as flexible crown ether moieties, facilitate the creation of a soft shell around the dimers of organic cations, which efficiently reduces strains that appear in the crystals in the course of the structural photo-transformation of the main components.

Protonated styrylpyridines were found to be prone to the formation of crystals with a high degree of disorder or of low-symmetry crystals of poor quality, which contain a large number of crystallographically independent formula units and are characterized by incomplete occupancy of

positions. Such crystals are best described by structures of supramolecular assemblies that are formed in solution as a result of self-assembly.

The approach, which we developed in terms of the crystal design of specified packing of styrylheterocycles, is, on the whole, correct. Although the protonated forms of these compounds are somewhat less suitable for investigation of solid-state PCA reactions in single crystals compared to related styryl dyes, these compounds are much more promising in this respect than neutral styrylheterocycles.

## Experimental

The melting points (uncorrected) were measured in capillaries on a Mel-Temp II instrument. The  $^1\text{H}$  NMR spectra were

**Table 2.** Crystal parameters and the X-ray diffraction data collection and refinement statistics for compounds **1b**, **7b**·0.5C<sub>6</sub>H<sub>6</sub>, **2b**, and **2b/11**

Parameter	<b>1b</b>	<b>7b</b> ·0.5C <sub>6</sub> H <sub>6</sub>	<b>2b</b>	<b>2b/11</b>
Molecular formula	C <sub>13</sub> H <sub>12</sub> ClNO <sub>4</sub>	C <sub>16</sub> H <sub>13</sub> Cl <sub>3</sub> NO <sub>4</sub>	C <sub>13</sub> H <sub>11</sub> ClN <sub>2</sub> O <sub>6</sub>	C <sub>26</sub> H <sub>22</sub> Cl <sub>2</sub> N <sub>4</sub> O <sub>12</sub>
Molecular weight/g mol <sup>-1</sup>	281.69	389.62	326.69	653.38
Crystal system	Monoclinic	Monoclinic	Monoclinic	Monoclinic
Space group	C2/c	P2 <sub>1</sub> /n	P2 <sub>1</sub> /n	P2 <sub>1</sub> /n
a/Å	9.8873(3)	21.9866(19)	7.9262(3)	7.684(3)
b/Å	12.6317(4)	17.5923(15)	13.8640(6)	14.157(5)
c/Å	19.9393(6)	36.269(3)	12.9850(5)	13.004(4)
α/deg	90	90	90	90
β/deg	92.1200(10)	106.924(4)	101.976(2)	102.453(6)
γ/deg	90	90	90	90
V/Å <sup>3</sup>	2488.58(13)	13421(2)	1395.85(10)	1381.3(8)
Z	8	32	4	2
ρ <sub>calc</sub> /g cm <sup>-3</sup>	1.504	1.543	1.555	1.571
F(000)	1168	6368	672	672
μ(Mo/Kα)/mm <sup>-1</sup>	0.317	0.566	0.306	0.309
Crystal dimensions/mm	0.26×0.14×0.14	0.24×0.20×0.14	0.64×0.24×0.09	0.64×0.24×0.09
Scan mode/θ-Scanning range/deg	ω/2.78–29.00	ω/1.27–29.00	ω/2.78–30.00	ω/2.84–28.98
Ranges of reflection indices	–13 ≤ h ≤ 13, –13 ≤ k ≤ 17, –27 ≤ l ≤ 27	–27 ≤ h ≤ 29, –24 ≤ k ≤ 24, –49 ≤ l ≤ 46	–11 ≤ h ≤ 11, –19 ≤ k ≤ 15, –18 ≤ l ≤ 17	–10 ≤ h ≤ 10, –19 ≤ k ≤ 9, –13 ≤ l ≤ 17
Number of measured reflections	7703	114407	8725	7918
Number of independent reflections ( <i>R</i> <sub>int</sub> )	3279 (0.0229)	35330 (0.5339)	3956 (0.0204)	3566 (0.1052)
Number of reflections with <i>I</i> > 2σ( <i>I</i> )	2701	5951	3055	1433
Number of refinement variables	299	1729	243	390
<i>R</i> Factors based on reflections with <i>I</i> > 2σ( <i>I</i> )				
<i>R</i> <sub>1</sub>	0.0363	0.1042	0.0509	0.1216
<i>wR</i> <sub>2</sub>	0.1009	0.2227	0.1306	0.3038
based on all reflections				
<i>R</i> <sub>1</sub>	0.0460	0.4625	0.0684	0.2583
<i>wR</i> <sub>2</sub>	0.1062	0.3044	0.1455	0.3397
Goodness-of-fit on <i>F</i> <sup>2</sup>	1.074	0.705	1.025	1.010
Residual electron density (min/max), e/Å <sup>3</sup>	–0.386/0.312	–0.888/2.037	–0.629/0.976	–0.541/0.451

recorded on a Bruker DRX500 spectrometer (500.13 MHz) in DMSO- $d_6$  at 25–30 °C with the use of the solvent as the internal standard ( $\delta_H$  2.50). The chemical shifts and the spin-spin coupling constants were measured with an accuracy of 0.01 ppm and 0.1 Hz, respectively. The absorption spectra of solutions ( $C = 5 \cdot 10^{-5}$  mol L $^{-1}$ ) in acetonitrile were recorded on a UV-3101PC spectrophotometer (Shimadzu) in the region of 200–600 nm (with 1 nm sampling interval) in 1 cm quartz cells. The elemental analysis was carried out in the Laboratory of Microanalysis of the A. N. Nesmeyanov Institute of Organoelement Compounds of the Russian Academy of Sciences (Moscow) using samples dried *in vacuo* at 60 °C.

Neutral styrylpyridines, *viz.*, 4-[(*E*)-1-ethenyl-2-phenyl]pyridine, 4-[(*E*)-1-ethenyl-2-(4-nitrophenyl)]pyridine, 4-[(*E*)-2-[4-(dimethylamino)phenyl]-1-ethenyl]pyridine, 4-[(*E*)-1-ethenyl-2-(4-methoxyphenyl)]pyridine, 4-[(*E*)-1-ethenyl-2-[4-(methylsulfanyl)phenyl]]pyridine, 4-[(*E*)-2-(3,4-dimethoxyphenyl)-1-ethenyl]pyridine, 4-[(*E*)-2-(3,4-dichlorophenyl)-1-ethenyl]pyridine, 4-[(*E*)-2-(2,3,5,6,8,9,11,12-octahydrobenzo-1,4,7,10,13-pentaoxacyclopentadecin-15-yl)-1-ethenyl]pyridine, and 4-[(*E*)-2-(2,3,5,6,8,9,11,12,14,15-decahydro-

1,4,7,10,13,16-benzohexaoxacyclooctadecin-18-yl)-1-ethenyl]pyridine, were synthesized according to known methods;<sup>1,20,23</sup> 70% HClO $_4$  (Aldrich) was used without additional purification.

**Synthesis of styrylpyridine hydropchlorates 1b–9b (general procedure).** To a solution of neutral 4-styrylpyridine (0.60 mmol) in acetonitrile (2 mL), 70% HClO $_4$  (62  $\mu$ L, 0.72 mmol) was added. The reaction mixture was diluted with 30 mL of benzene (benzene–hexane mixture (2 : 1) for **7b** and **9b**) and cooled to 5 °C. The precipitate that formed was filtered off, washed with distilled water (2  $\times$  2 mL), and dried in air in the dark.

**4-[(*E*)-1-Ethenyl-2-phenyl]pyridinium perchlorate (1b).** Pale-yellow powder (yield 89%), m.p. 228–230 °C. Found (%): C, 55.25; H, 4.17; N, 4.96. C $_{13}$ H $_{12}$ ClNO $_4$ . Calculated (%): C, 55.43; H, 4.29; N, 4.97.  $^1$ H NMR,  $\delta$ : 7.45 (t, 1 H, H(4'),  $J = 7.3$  Hz); 7.50 (t, 2 H, H(3'), H(5'),  $J = 7.3$  Hz); 7.54 (d, 1 H, CH=CHPy,  $J = 16.6$  Hz); 7.76 (d, 2 H, H(2'), H(6'),  $J = 6.8$  Hz); 7.99 (d, 1 H, CH=CHPy,  $J = 16.6$  Hz); 8.18 (d, 2 H, H(3), H(5),  $J = 6.4$  Hz); 8.83 (d, 2 H, H(2), H(6),  $J = 6.4$  Hz). UV (MeCN),  $\lambda_{\max}/\epsilon$ : 343 (30300).

**4-[(*E*)-1-Ethenyl-2-(4-nitrophenyl)]pyridinium perchlorate (2b).** Pale-brown powder (yield 49%), m.p. > 250 °C (with de-

**Table 3.** Crystal parameters and the X-ray diffraction data collection and refinement statistics for compounds **3b**·0.5C $_6$ H $_6$ , **4b**, and **4b**·0.5C $_6$ H $_6$

Parameter	<b>3b</b> ·0.5C $_6$ H $_6$	<b>4b</b>	<b>4b</b> ·0.5C $_6$ H $_6$
Molecular formula	C $_{18}$ H $_{20}$ ClN $_2$ O $_4$	C $_{14}$ H $_{14}$ ClNO $_5$	C $_{17}$ H $_{17}$ ClNO $_5$
Molecular weight/g mol $^{-1}$	363.81	311.71	350.77
Crystal system	Triclinic	Triclinic	Triclinic
Space group	$P\bar{1}$	$P\bar{1}$	$P\bar{1}$
$a/\text{\AA}$	6.8729(2)	8.4042(14)	6.7884(2)
$b/\text{\AA}$	15.7931(4)	8.8189(15)	9.1562(3)
$c/\text{\AA}$	18.0432(5)	10.4718(19)	13.4368(4)
$\alpha/\text{deg}$	67.8120(10)	77.185(2)	79.2000(10)
$\beta/\text{deg}$	79.3560(10)	87.499(3)	89.7030(10)
$\gamma/\text{deg}$	88.4630(10)	66.431(2)	81.6910(10)
$V/\text{\AA}^3$	1780.28(8)	692.8(2)	811.57(4)
$Z$	4	2	2
$\rho_{\text{calc}}/\text{g cm}^{-3}$	1.357	1.494	1.435
$F(000)$	764	324	366
$\mu(\text{Mo}/K\alpha)/\text{mm}^{-1}$	0.240	0.297	0.263
Crystal dimensions/mm	0.36 $\times$ 0.22 $\times$ 0.18	0.29 $\times$ 0.12 $\times$ 0.04	0.28 $\times$ 0.20 $\times$ 0.12
Scan mode/ $\theta$ -Scanning range/deg	$\omega/1.24$ –29.00	$\omega/2.00$ –29.00	$\omega/1.54$ –29.00
Ranges of reflection indices	$-5 \leq h \leq 9$ , $-21 \leq k \leq 21$ , $-24 \leq l \leq 22$	$-11 \leq h \leq 11$ , $-12 \leq k \leq 11$ , $-14 \leq l \leq 14$	$-9 \leq h \leq 9$ , $-12 \leq k \leq 12$ , $-18 \leq l \leq 18$
Number of measured reflections	15674	7702	8528
Number of independent reflections ( $R_{\text{int}}$ )	9131 (0.0321)	3680 (0.0333)	4274 (0.0164)
Number of reflections with $I > 2\sigma(I)$	7184	2648	3699
Number of refinement variables	670	300	394
$R$ Factors based on reflections with $I > 2\sigma(I)$			
$R_1$	0.0647	0.0461	0.0312
$wR_2$	0.1736	0.1079	0.0898
based on all reflections			
$R_1$	0.0830	0.0686	0.0375
$wR_2$	0.1858	0.1164	0.0935
Goodness-of-fit on $F^2$	1.046	1.009	1.065
Residual electron density (min/max), e/ $\text{\AA}^3$	–0.535/0.695	–0.388/0.293	–0.336/0.296

comp.). Found (%): C, 47.85; H, 3.35; N, 8.54.  $C_{13}H_{11}ClN_2O_6$ . Calculated (%): C, 47.79; H, 3.39; N, 8.58.  $^1H$  NMR,  $\delta$ : 7.74 (d, 1 H,  $CH=CHPy$ ,  $J = 16.6$  Hz); 8.00 (d, 2 H,  $H(2')$ ,  $H(6')$ ,  $J = 8.6$  Hz); 8.06 (d, 1 H,  $CH=CHPy$ ,  $J = 16.6$  Hz); 8.20 (d, 2 H,  $H(3)$ ,  $H(5)$ ,  $J = 6.8$  Hz); 8.34 (d, 2 H,  $H(3')$ ,  $H(5')$ ,  $J = 8.6$  Hz); 8.88 (d, 2 H,  $H(2)$ ,  $H(6)$ ,  $J = 6.8$  Hz). UV (MeCN),  $\lambda_{max}/nm$  ( $\epsilon$ ): 340 (33100).

**4-[(E)-2-[4-(Dimethylamino)phenyl]-1-ethenyl]pyridinium perchlorate (3b)**. Red-brown crystals (yield 71%), m.p. 221–223 °C (with decomp.). Found (%): C, 56.28; H, 5.53; N, 7.86.  $C_{15}H_{17}ClN_2O_4 \cdot 0.3C_6H_6 \cdot 0.6H_2O$ . Calculated (%): C, 56.21; H, 5.62; N, 7.80.  $^1H$  NMR,  $\delta$ : 3.02 (s, 6 H,  $NMe_2$ ); 6.79 (d, 2 H,  $H(3')$ ,  $H(5')$ ,  $J = 8.9$  Hz); 7.19 (d, 1 H,  $CH=CHPy$ ,  $J = 16.1$  Hz); 7.60 (d, 2 H,  $H(2')$ ,  $H(6')$ ,  $J = 8.9$  Hz); 7.90 (d, 1 H,  $CH=CHPy$ ,  $J = 16.1$  Hz); 8.02 (d, 2 H,  $H(3)$ ,  $H(5)$ ,  $J = 6.6$  Hz); 8.67 (d, 2 H,  $H(2)$ ,  $H(6)$ ,  $J = 6.6$  Hz). UV (MeCN),  $\lambda_{max}/nm$  ( $\epsilon$ ): 470 (36700).

**4-[(E)-1-Ethenyl-2-(4-methoxyphenyl)]pyridinium perchlorate (4b)**. Pale-yellow powder (yield 56%), m.p. 228–231 °C (with decomp.). Found (%): C, 53.97; H, 4.49; N, 4.48.  $C_{14}H_{14}ClNO_5$ . Calculated (%): C, 53.94; H, 4.53; N, 4.49.  $^1H$  NMR,  $\delta$ : 3.83 (s, 3 H,  $OMe$ ); 7.06 (d, 2 H,  $H(3')$ ,  $H(5')$ ,

$J = 8.8$  Hz); 7.37 (d, 1 H,  $CH=CHPy$ ,  $J = 16.4$  Hz); 7.72 (d, 2 H,  $H(2')$ ,  $H(6')$ ,  $J = 8.8$  Hz); 7.95 (d, 1 H,  $CH=CHPy$ ,  $J = 16.4$  Hz); 8.12 (d, 2 H,  $H(3)$ ,  $H(5)$ ,  $J = 6.8$  Hz); 8.78 (d, 2 H,  $H(2)$ ,  $H(6)$ ,  $J = 6.8$  Hz). UV (MeCN),  $\lambda_{max}/nm$  ( $\epsilon$ ): 380 (31100).

**4-[(E)-2-[1-Ethenyl-4-(methylsulfanyl)phenyl]]pyridinium perchlorate (5b)**. Yellow powder (yield 73%), m.p. 228–230 °C (with decomp.). Found (%): C, 51.28; H, 4.35; N, 4.21.  $C_{14}H_{14}ClNO_4S$ . Calculated (%): C, 51.30; H, 4.31; N, 4.27.  $^1H$  NMR,  $\delta$ : 2.53 (s, 3 H,  $SMe$ ); 7.36 (d, 2 H,  $H(3')$ ,  $H(5')$ ,  $J = 8.3$  Hz); 7.47 (d, 1 H,  $CH=CHPy$ ,  $J = 16.4$  Hz); 7.69 (d, 2 H,  $H(2')$ ,  $H(6')$ ,  $J = 8.3$  Hz); 7.93 (d, 1 H,  $CH=CHPy$ ,  $J = 16.4$  Hz); 8.12 (d, 2 H,  $H(3)$ ,  $H(5)$ ,  $J = 6.3$  Hz); 8.79 (d, 2 H,  $H(2)$ ,  $H(6)$ ,  $J = 6.3$  Hz). UV (MeCN),  $\lambda_{max}/nm$  ( $\epsilon$ ): 392 (32500).

**4-[(E)-2-(3,4-Dimethoxyphenyl)-1-ethenyl]pyridinium perchlorate (6b)**. Yellow powder (yield 90%), m.p. 260–262 °C (with decomp.). Found (%): C, 50.81; H, 4.69; N, 3.91.  $C_{15}H_{16}ClNO_6 \cdot 0.75H_2O$ . Calculated (%): C, 50.71; H, 4.97; N, 3.94.  $^1H$  NMR,  $\delta$ : 3.82 (s, 3 H,  $OMe$ ); 3.85 (s, 3 H,  $OMe$ ); 7.06 (d, 1 H,  $H(5')$ ,  $J = 8.4$  Hz); 7.29 (dd, 1 H,  $H(6')$ ,  $J = 8.4$  Hz,  $J = 1.8$  Hz); 7.39 (d, 1 H,  $H(2')$ ,  $J = 1.8$  Hz); 7.40 (d, 1 H,  $CH=CHPy$ ,  $J = 16.4$  Hz); 7.91 (d, 1 H,  $CH=CHPy$ ,  $J = 16.4$  Hz);

**Table 4.** Crystal parameters and the X-ray diffraction data collection and refinement statistics for compounds **5b** and **5b**·0.76C<sub>6</sub>H<sub>6</sub>·0.14H<sub>2</sub>O, **6b<sup>m</sup>** and **6b<sup>o</sup>**

Parameter	<b>5b</b>	<b>5b</b> ·0.76C <sub>6</sub> H <sub>6</sub> ·0.14H <sub>2</sub> O	<b>6b<sup>m</sup></b>	<b>6b<sup>o</sup></b>
Molecular formula	C <sub>14</sub> H <sub>14</sub> ClNO <sub>4</sub> S	C <sub>18.57</sub> H <sub>18.86</sub> ClNO <sub>4.14</sub> S	C <sub>15</sub> H <sub>16</sub> ClNO <sub>6</sub>	C <sub>15</sub> H <sub>16</sub> ClNO <sub>6</sub>
Molecular weight/g mol <sup>−1</sup>	327.77	389.86	341.74	341.74
Crystal system	Triclinic	Triclinic	Monoclinic	Orthorhombic
Space group	<i>P</i> $\bar{1}$	<i>P</i> $\bar{1}$	<i>C</i> 2/ <i>c</i>	<i>Pca</i> 2 <sub>1</sub>
<i>a</i> /Å	8.0773(14)	14.764(4)	18.7653(5)	34.351(4)
<i>b</i> /Å	9.6610(16)	25.923(6)	13.4602(4)	4.9898(5)
<i>c</i> /Å	10.0253(17)	27.154(7)	12.5863(4)	8.9617(10)
$\alpha$ /deg	93.815(7)	81.782(9)	90	90
$\beta$ /deg	101.120(7)	77.770(11)	109.8750(10)	90
$\gamma$ /deg	106.520(6)	86.951(10)	90	90
<i>V</i> /Å <sup>3</sup>	729.8(2)	10049(4)	2989.75(15)	1536.1(3)
<i>Z</i>	2	21	8	4
$\rho_{calc}/g\ cm^{-3}$	1.492	1.353	1.518	1.478
<i>F</i> (000)	340	4272	1424	712
$\mu(Mo/K\alpha)/mm^{-1}$	0.419	0.332	0.288	0.280
Crystal dimensions/mm	0.24×0.22×0.16	0.60×0.08×0.03	0.24×0.22×0.20	0.60×0.12×0.08
Scan mode/ $\theta$ -Scanning range/deg	$\omega/2.09$ –29.00	$\omega/1.18$ –29.00	$\omega/1.90$ –29.00	$\omega/1.19$ –28.50
Ranges of reflection indices	$-11 \leq h \leq 10$ , $-13 \leq k \leq 13$ , $-13 \leq l \leq 13$	$-18 \leq h \leq 20$ , $-32 \leq k \leq 35$ , $-36 \leq l \leq 37$	$-25 \leq h \leq 25$ , $-18 \leq k \leq 17$ , $-17 \leq l \leq 17$	$-46 \leq h \leq 31$ , $-6 \leq k \leq 6$ , $-9 \leq l \leq 12$
Number of measured reflections	5986	84512	15638	8231
Number of independent reflections ( <i>R</i> <sub>int</sub> )	3770 (0.0565)	52435 (0.4538)	3980 (0.0258)	3535 (0.0592)
Number of reflections with <i>I</i> > 2 $\sigma$ ( <i>I</i> )	2081	5001	3291	2302
Number of refinement variables	194	865	337	208
<i>R</i> Factors based on reflections with <i>I</i> > 2 $\sigma$ ( <i>I</i> )				
<i>R</i> <sub>1</sub>	0.0926	0.1973	0.0393	0.1089
<i>wR</i> <sub>2</sub>	0.2975	0.3672	0.1081	0.2944
based on all reflections				
<i>R</i> <sub>1</sub>	0.1432	0.6555	0.0489	0.1565
<i>wR</i> <sub>2</sub>	0.3133	0.5165	0.1142	0.3444
Goodness-of-fit on <i>F</i> <sup>2</sup>	1.104	0.764	1.044	1.237
Residual electron density (min/max), e/Å <sup>3</sup>	−0.790/0.876	−0.669/1.769	−0.369/0.449	−0.654/1.458



8.09 (d, 2 H, H(3), H(5),  $J = 6.1$  Hz); 8.76 (d, 2 H, H(2), H(6),  $J = 6.1$  Hz). UV (MeCN),  $\lambda_{\text{max}}/\text{nm}$  ( $\epsilon$ ): 395 (29200).

**4-[(E)-2-(3,4-Dichlorophenyl)-1-ethenyl]pyridinium perchlorate (7b).** White powder (yield 76%), m.p. 210–212 °C. Found (%): C, 44.51; H, 2.73; N, 3.91.  $\text{C}_{13}\text{H}_{10}\text{Cl}_2\text{NO}_4$ . Calculated (%): C, 44.54; H, 2.88; N, 4.00.  $^1\text{H}$  NMR,  $\delta$ : 7.64 (d, 1 H,  $\text{CH}=\text{CHPy}$ ,  $J = 16.4$  Hz); 7.71 (dd, 1 H, H(6'),  $J = 8.4$  Hz,  $J = 1.8$  Hz); 7.76 (d, 1 H, H(5'),  $J = 8.4$  Hz); 7.92 (d, 1 H,  $\text{CH}=\text{CHPy}$ ,  $J = 16.4$  Hz); 8.04 (d, 1 H, H(2'),  $J = 1.8$  Hz); 8.13 (d, 2 H, H(3), H(5),  $J = 6.6$  Hz); 8.86 (d, 2 H, H(2), H(6),  $J = 6.6$  Hz). UV (MeCN),  $\lambda_{\text{max}}/\text{nm}$  ( $\epsilon$ ): 339 (32100).

**4-[(E)-2-(2,3,5,6,8,9,11,12-Octahydro-1,4,7,10,13-benzopentaoxacycloptadecin-15-yl)-1-ethenyl]pyridinium perchlorate (8b).** Yellow powder (yield 70%), m.p. 242–244 °C. Found (%): C, 53.59; H, 5.68; N, 2.79.  $\text{C}_{24}\text{H}_{26}\text{ClNO}_9$ . Calculated (%): C, 53.45; H, 5.55; N, 2.97.  $^1\text{H}$  NMR,  $\delta$ : 3.63 (m, 8 H, 4  $\text{CH}_2\text{O}$ ); 3.79 (m, 2 H, 4'- $\text{CH}_2\text{CH}_2\text{OAr}$ ); 3.81 (m, 2 H, 3'- $\text{CH}_2\text{CH}_2\text{OAr}$ ); 4.12 (m, 2 H, 4'- $\text{CH}_2\text{OAr}$ ); 4.14 (m, 2 H, 3'- $\text{CH}_2\text{OAr}$ ); 7.05 (d, 1 H, H(5'),  $J = 8.3$  Hz); 7.28 (br.d, 1 H, H(6'),  $J = 8.3$  Hz); 7.38 (d, 1 H,  $\text{CH}=\text{CHPy}$ ,  $J = 16.3$  Hz); 7.40 (br.s, 1 H, H(2')); 7.88 (d, 1 H,  $\text{CH}=\text{CHPy}$ ,  $J = 16.3$  Hz); 8.06 (d, 2 H, H(3),

H(5),  $J = 6.5$  Hz); 8.76 (d, 2 H, H(2), H(6),  $J = 6.5$  Hz). UV (MeCN),  $\lambda_{\text{max}}/\text{nm}$  ( $\epsilon$ ): 394 (26500).

**4-[(E)-2-(2,3,5,6,8,9,11,12,14,15-Decahydro-1,4,7,10,13,16-benzohexaoxacyclooctadecin-18-yl)-1-ethenyl]pyridinium perchlorate (9b).** Yellow powder (yield 95%), m.p. 233–235 °C (with decomp.). Found (%): C, 51.90; H, 6.11; N, 2.63.  $\text{C}_{23}\text{H}_{30}\text{ClNO}_{10} \cdot \text{H}_2\text{O}$ . Calculated (%): C, 51.74; H, 6.04; N, 2.62.  $^1\text{H}$  NMR,  $\delta$ : 3.53 (s, 4 H, 2  $\text{CH}_2\text{O}$ ); 3.57 (m, 4 H, 2  $\text{CH}_2\text{O}$ ); 3.62 (m, 4 H, 2  $\text{CH}_2\text{O}$ ); 3.77 (m, 2 H, 4'- $\text{CH}_2\text{CH}_2\text{OAr}$ ); 3.80 (m, 2 H, 3'- $\text{CH}_2\text{CH}_2\text{OAr}$ ); 4.15 (m, 2 H, 4'- $\text{CH}_2\text{OAr}$ ); 4.18 (m, 2 H, 3'- $\text{CH}_2\text{OAr}$ ); 7.06 (d, 1 H, H(5'),  $J = 8.3$  Hz); 7.27 (dd, 1 H, H(6'),  $J = 8.3$  Hz,  $J = 1.5$  Hz); 7.39 (d, 1 H,  $\text{CH}=\text{CHPy}$ ,  $J = 16.3$  Hz); 7.39 (d, 1 H, H(2'),  $J = 1.5$  Hz); 7.89 (d, 1 H,  $\text{CH}=\text{CHPy}$ ,  $J = 16.3$  Hz); 8.07 (d, 2 H, H(3), H(5),  $J = 6.4$  Hz); 8.76 (d, 2 H, H(2), H(6),  $J = 6.4$  Hz). UV (MeCN),  $\lambda_{\text{max}}/\text{nm}$  ( $\epsilon$ ): 389 (26800).

#### Synthesis of cyclobutane derivatives from hydrop perchlorates

**1b–9b (general procedure).** Benzene (0.3 mL) was added to a solution of compounds **1b–9b** (0.1 mmol) in MeCN (0.5–1 mL). The reaction mixture was concentrated in a 10-cm Petri dish to form a polycrystalline film of the corresponding compound. The

**Table 5.** Crystal parameters and the X-ray diffraction data collection and refinement statistics for compounds **8b**·0.5 $\text{C}_6\text{H}_6$ ·0.125 $\text{H}_2\text{O}$ , (**8b/13**)· $\text{C}_6\text{H}_6$ ·0.25 $\text{H}_2\text{O}$ , and **13**· $\text{C}_6\text{H}_6$ ·0.25 $\text{H}_2\text{O}$

Parameter	<b>8b</b> ·0.5 $\text{C}_6\text{H}_6$ ·0.125 $\text{H}_2\text{O}$	( <b>8b/13</b> )· $\text{C}_6\text{H}_6$ ·0.25 $\text{H}_2\text{O}$	<b>13</b> · $\text{C}_6\text{H}_6$ ·0.25 $\text{H}_2\text{O}$
Molecular formula	$\text{C}_{24}\text{H}_{29.25}\text{ClNO}_{9.13}$	$\text{C}_{48}\text{H}_{58.5}\text{Cl}_2\text{N}_2\text{O}_{18.25}$	$\text{C}_{48}\text{H}_{58.5}\text{Cl}_2\text{N}_2\text{O}_{18.25}$
Molecular weight/g mol <sup>−1</sup>	513.18	1026.37	1026.37
Crystal system	Triclinic	Triclinic	Triclinic
Space group	$P\bar{1}$	$P\bar{1}$	$P\bar{1}$
$a/\text{\AA}$	11.9327(16)	11.911(2)	15.8911(8)
$b/\text{\AA}$	12.7937(16)	12.921(2)	16.2070(8)
$c/\text{\AA}$	16.551(2)	16.348(3)	19.3135(9)
$\alpha/\text{deg}$	79.986(7)	79.280(9)	80.241(3)
$\beta/\text{deg}$	88.423(6)	88.087(8)	85.211(3)
$\gamma/\text{deg}$	77.531(6)	77.918(8)	79.987(3)
$V/\text{\AA}^3$	2429.4(5)	2417.2(7)	4820.0(4)
$Z$	4	2	4
$\rho_{\text{calc}}/\text{g cm}^{-3}$	1.403	1.410	1.414
$F(000)$	1081	1081	2162
$\mu(\text{Mo}/K\alpha)/\text{mm}^{-1}$	0.212	0.213	0.214
Crystal dimensions/mm	0.46×0.08×0.06	0.46×0.08×0.06	0.12×0.08×0.06
Scan mode/ $\theta$ -Scanning range/deg	$\omega/1.25$ –29.00	$\omega/1.64$ –29.00	$\omega/1.29$ –18.96
Ranges of reflection indices	$-16 \leq h \leq 16$ , $-17 \leq k \leq 17$ , $-22 \leq l \leq 21$	$-16 \leq h \leq 16$ , $-17 \leq k \leq 17$ , $-22 \leq l \leq 22$	$-14 \leq h \leq 14$ , $-14 \leq k \leq 14$ , $-17 \leq l \leq 17$
Number of measured reflections	27380	30211	26012
Number of independent reflections ( $R_{\text{int}}$ )	12822 (0.1885)	12716 (0.3006)	7502 (0.0481)
Number of reflections with $I > 2\sigma(I)$	2882	2428	5670
Number of refinement variables	807	768	1343
$R$ Factors based on reflections with $I > 2\sigma(I)$			
$R_1$	0.0929	0.1152	0.1021
$wR_2$	0.1704	0.1862	0.2630
based on all reflections			
$R_1$	0.3676	0.4262	0.1295
$wR_2$	0.2198	0.2459	0.2802
Goodness-of-fit on $F^2$	0.787	0.783	1.089
Residual electron density (min/max), $\text{e}/\text{\AA}^3$	−0.247/0.384	−0.278/0.322	−0.316/0.734

sample was irradiated with unfiltered light using a 60 W incandescent lamp at a distance of 15 cm for 20–200 h. The resulting compounds were collected mechanically. The compositions of the products and the degree of conversion into cyclobutane derivatives were analyzed based on the  $^1\text{H}$  NMR spectroscopic data (in  $\text{DMSO-d}_6$ ) by comparing the integrated intensities of the signals for protons. The experimental data obtained at different exposure times are given in Table 1. In the cases when the degree of conversion was  $\geq 95\%$ , the characteristics of the resulting cyclobutane derivatives are given.

***r*-4-[*c*-2,*t*-4-Diphenyl-*t*-3-(pyridinio-4-yl)cyclobutyl]pyridinium diperchlorate (*rcft*-10)** was synthesized after irradiation for 50 h as a white powder, m.p. 269–270 °C (with decomp.). Found (%): C, 55.37; H, 4.21; N, 4.91.  $\text{C}_{26}\text{H}_{24}\text{Cl}_2\text{N}_2\text{O}_8$ . Calculated (%): C, 55.43; H, 4.29; N, 4.97.  $^1\text{H}$  NMR,  $\delta$ : 4.87 (dd, 2 H, 2  $\text{CHAr}$ ,  $J = 9.4$  Hz,  $J = 7.4$  Hz); 4.95 (dd, 2 H, 2  $\text{CHPy}$ ,  $J = 9.4$  Hz,  $J = 7.4$  Hz); 7.12 (t, 2 H, 2  $\text{H}(4')$ ,  $J = 7.3$  Hz); 7.21 (t, 4 H, 2  $\text{H}(3')$ , 2  $\text{H}(5')$ ,  $J = 7.6$  Hz); 7.26 (d, 4 H, 2  $\text{H}(2')$ , 2  $\text{H}(6')$ ,  $J = 7.3$  Hz); 7.81 (d, 4 H, 2  $\text{H}(3)$ , 2  $\text{H}(5)$ ,  $J = 6.1$  Hz); 8.66 (d, 4 H, 2  $\text{H}(2)$ , 2  $\text{H}(6)$ ,  $J = 6.1$  Hz). UV (MeCN),  $\lambda_{\text{max}}/\text{nm}$  ( $\epsilon$ ): 255 (13300).

***r*-4-[*c*-2,*t*-4-Bis[4-(methylsulfanyl)phenyl]-*t*-3-(pyridinio-4-yl)cyclobutyl]pyridinium diperchlorate (*rcft*-12)** was synthesized

after irradiation for 20 h as a pale-yellow powder, m.p.  $> 214$  °C (with decomp.). Found (%): C, 49.97; H, 4.26; N, 4.17.  $\text{C}_{28}\text{H}_{28}\text{Cl}_2\text{N}_2\text{O}_8\text{S}_2 \cdot \text{H}_2\text{O}$ . Calculated (%): C, 49.93; H, 4.49; N, 4.16.  $^1\text{H}$  NMR,  $\delta$ : 2.38 (s, 6 H, 2 MeS); 4.80 (dd, 2 H, 2  $\text{CHAr}$ ,  $J = 9.1$  Hz,  $J = 6.4$  Hz); 4.86 (dd, 2 H, 2  $\text{CHPy}$ ,  $J = 9.1$  Hz,  $J = 6.4$  Hz); 7.08 (d, 4 H, 2  $\text{H}(3')$ , 2  $\text{H}(5')$ ,  $J = 8.2$  Hz); 7.20 (d, 4 H, 2  $\text{H}(2')$ , 2  $\text{H}(6')$ ,  $J = 8.2$  Hz); 7.76 (d, 4 H, 2  $\text{H}(3)$ , 2  $\text{H}(5)$ ,  $J = 5.9$  Hz); 8.67 (d, 4 H, 2  $\text{H}(2)$ , 2  $\text{H}(6)$ ,  $J = 5.9$  Hz). UV (MeCN),  $\lambda_{\text{max}}/\text{nm}$  ( $\epsilon$ ): 260 (31400).

***r*-4-[*c*-2,*t*-4-Bis(2,3,5,6,8,9,11,12-octahydro-1,4,7,10,13-benzopentaoxacyclopentadecin-15-yl)-*t*-3-(pyridinio-4-yl)cyclobutyl]pyridinium diperchlorate (*rcft*-13)** was synthesized after irradiation for 200 h as a pale-yellow powder, m.p.  $> 175$  °C (with decomp.). Found (%): C, 52.35; H, 5.47; N, 2.73.  $\text{C}_{42}\text{H}_{52}\text{Cl}_2\text{N}_2\text{O}_{18} \cdot \text{H}_2\text{O}$ . Calculated (%): C, 52.45; H, 5.66; N, 2.91.  $^1\text{H}$  NMR,  $\delta$ : 3.58 (m, 16 H, 8  $\text{CH}_2\text{O}$ ); 3.70 (m, 8 H, 4  $\text{CH}_2\text{CH}_2\text{OAr}$ ); 3.93 (m, 8 H, 4  $\text{CH}_2\text{OAr}$ ); 4.75 (dd, 2 H, 2  $\text{CHAr}$ ,  $J = 8.5$  Hz,  $J = 6.5$  Hz); 4.82 (dd, 2 H, 2  $\text{CHPy}$ ,  $J = 8.9$  Hz,  $J = 6.5$  Hz); 6.75 (d, 2 H, 2  $\text{H}(5')$ ,  $J = 8.3$  Hz); 6.77 (br.d, 2 H, 2  $\text{H}(6')$ ,  $J = 8.3$  Hz); 6.82 (br.s, 2 H, 2  $\text{H}(2')$ ); 7.79 (d, 4 H, 2  $\text{H}(3)$ , 2  $\text{H}(5)$ ,  $J = 5.8$  Hz); 8.68 (d, 4 H, 2  $\text{H}(2)$ , 2  $\text{H}(6)$ ,  $J = 5.8$  Hz). UV (MeCN),  $\lambda_{\text{max}}/\text{nm}$  ( $\epsilon$ ): 281 (7000).

**Table 6.** Crystal parameters and the X-ray diffraction data collection and refinement statistics for compounds **9b**  $\cdot$  MeCN  $\cdot$  0.5 $\text{C}_6\text{H}_6 \cdot \text{H}_2\text{O}$ , **9b**  $\cdot \text{NH}_4\text{ClO}_4$ , and **14**  $\cdot \text{NH}_4\text{ClO}_4 \cdot \text{H}_2\text{O}$

Parameter	<b>9b</b> $\cdot$ MeCN $\cdot$ 0.5 $\text{C}_6\text{H}_6 \cdot \text{H}_2\text{O}$	<b>9b</b> $\cdot \text{NH}_4\text{ClO}_4$	<b>14</b> $\cdot \text{NH}_4\text{ClO}_4 \cdot \text{H}_2\text{O}$
Molecular formula	$\text{C}_{28}\text{H}_{38}\text{ClN}_2\text{O}_{11}$	$\text{C}_{23}\text{H}_{34}\text{Cl}_2\text{N}_2\text{O}_{14}$	$\text{C}_{46}\text{H}_{70}\text{Cl}_4\text{N}_4\text{O}_{29}$
Molecular weight/g mol $^{-1}$	614.05	633.42	1284.86
Crystal system	Triclinic	Triclinic	Monoclinic
Space group	$P\bar{1}$	$P\bar{1}$	$P2_1/c$
$a/\text{\AA}$	7.691(2)	6.2285(6)	11.5375(4)
$b/\text{\AA}$	13.959(4)	12.3326(11)	10.8660(4)
$c/\text{\AA}$	14.546(4)	19.1841(16)	22.8582(8)
$\alpha/\text{deg}$	77.688(5)	82.251(4)	90
$\beta/\text{deg}$	84.591(5)	84.565(4)	99.5780(10)
$\gamma/\text{deg}$	78.839(5)	76.145(3)	90
$V/\text{\AA}^3$	1494.7(7)	1414.7(2)	2825.70(17)
$Z$	2	2	2
$\rho_{\text{calc}}/\text{g cm}^{-3}$	1.364	1.487	1.510
$F(000)$	650	664	1348
$\mu(\text{Mo}/K\alpha)/\text{mm}^{-1}$	0.190	0.302	0.305
Crystal dimensions/mm	0.22 $\times$ 0.12 $\times$ 0.10	0.24 $\times$ 0.20 $\times$ 0.08	0.29 $\times$ 0.22 $\times$ 0.06
Scan mode/ $\theta$ -Scanning range/deg	$\omega/1.87$ –29.00	$\omega/1.07$ –25.00	$\omega/1.79$ –29.00
Ranges of reflection indices	$-10 \leq h \leq 10$ , $-19 \leq k \leq 18$ , $-19 \leq l \leq 19$	$-7 \leq h \leq 5$ , $-14 \leq k \leq 14$ , $-22 \leq l \leq 19$	$-15 \leq h \leq 15$ , $-14 \leq k \leq 14$ , $-31 \leq l \leq 31$
Number of measured reflections	14598	6705	34280
Number of independent reflections ( $R_{\text{int}}$ )	7647 (0.0670)	4748 (0.0728)	7517 (0.0471)
Number of reflections with $I > 2\sigma(I)$	3977	2320	5077
Number of refinement variables	500	408	681
$R$ Factors based on reflections with $I > 2\sigma(I)$			
$R_1$	0.0674	0.0921	0.0744
$wR_2$	0.1466	0.1737	0.1901
based on all reflections			
$R_1$	0.1363	0.2007	0.1105
$wR_2$	0.1702	0.2049	0.2049
Goodness-of-fit on $F^2$	0.933	0.963	1.040
Residual electron density (min/max), $\text{e}/\text{\AA}^3$	–0.354/0.282	–0.428/0.578	–0.468/0.667

***r*-4-[*c*-2,*t*-4-Bis(2,3,5,6,8,9,11,12,14,15-decahydro-1,4,7,10,13,16-benzohexaoxacyclooctadecin-18-yl)-*t*-3-(pyridinio-4-yl)cyclobutyl]pyridinium diperchlorate (*rectt*-14)** was synthesized after irradiation for 20 h as a yellowish powder, m.p. 263–265 °C (with decomp.). Found (%): C, 53.39; H, 5.75; N, 2.84.  $C_{46}H_{60}Cl_2N_2O_{20}$ . Calculated (%): C, 53.54; H, 5.86; N, 2.72.  $^1H$  NMR,  $\delta$ : 3.51 (s, 8 H, 4  $CH_2O$ ); 3.52–3.60 (m, 16 H, 8  $CH_2O$ ); 3.68 (m, 8 H, 4  $CH_2CH_2OAr$ ); 3.95 (m, 8 H, 4  $CH_2OAr$ ); 4.70 (dd, 2 H, 2  $CHAr$ ,  $J = 9.5$  Hz,  $J = 5.9$  Hz); 4.76 (dd, 2 H, 2  $CHPy$ ,  $J = 9.5$  Hz,  $J = 5.9$  Hz); 6.76 (s, 4 H, 2 H(5'), 2 H(6')); 6.80 (s, 2 H, 2 H(2')); 7.68 (br.s, 4 H, 2 H(3), 2 H(5)); 8.62 (br.s, 4 H, 2 H(2), 2 H(6)). UV (MeCN),  $\lambda_{max}/nm$  ( $\epsilon$ ): 283 (7500).

**X-ray diffraction study.** Single crystals of all compounds were mounted on a Bruker SMART-CCD or Bruker Microstar diffractometer under a cold nitrogen stream ( $T = 150(2)$  K for **4b** and **9b**·MeCN·0.5 $C_6H_6$ ·H $_2$ O and 120.0(2) K for the other compounds). The unit cell parameters were measured and the X-ray diffraction data sets were collected using Mo-K $\alpha$  radiation ( $\lambda = 0.71073$  Å, graphite monochromator,  $\omega$ -scan mode) on the Bruker SMART-CCD diffractometer or Cu-K $\alpha$  radiation ( $\lambda = 1.54184$  Å, graphite monochromator,  $\omega$ -scan mode) on the Bruker Microstar diffractometer. The X-ray diffraction data were processed with the use of the SAINT program.<sup>45</sup> All structures were solved by direct methods and refined by the least-squares method with anisotropic displacement parameters for nonhydrogen atoms. The exceptions were the oxygen atoms of the disordered perchlorate anions in the structures of **3b**·0.5 $C_6H_6$ , **13**· $C_6H_6$ ·0.25H $_2$ O, and **14**·NH $_4$ ClO $_4$ ·H $_2$ O, the atoms of the disordered pyridinium moieties in the structure of (**8b**/**13**)· $C_6H_6$ ·0.25H $_2$ O, and the whole structure of **5b**·0.76 $C_6H_6$ ·0.14H $_2$ O, whose non-hydrogen atoms were refined isotropically. The hydrogen atoms at the C atoms were positioned geometrically and refined isotropically in the structures of **2b**, **4b**, and **4b**·0.5 $C_6H_6$  (for the ordered groups), **6b<sup>m</sup>** (for the ordered groups) or using a riding model for the other structures. The hydrogen atoms at the N atoms of the pyridinium moieties were positioned geometrically and refined isotropically in the structures of **2b**, **4b**, **3b**·0.5 $C_6H_6$  (the ordered cation and the major *s* conformer of the disordered cation), **5b**, **9b**·MeCN·0.5 $C_6H_6$ ·H $_2$ O, and **9b**·NH $_4$ ClO $_4$  or using a riding model for the other structures. The hydrogen atoms of the NH $_4^+$  ions in the structures of **9b**·NH $_4$ ClO $_4$  and **14**·NH $_4$ ClO $_4$ ·H $_2$ O, the hydrogen atoms of the solvent water molecule in the structure of **9b**·MeCN·0.5 $C_6H_6$ ·H $_2$ O, and one of the hydrogen atoms of the solvent water molecule in the structure of **14**·NH $_4$ ClO $_4$ ·H $_2$ O were located in difference Fourier maps and refined isotropically. The second hydrogen atom of the water molecule in the structure of **14**·NH $_4$ ClO $_4$ ·H $_2$ O and all H atoms of the solvent water molecules in the structures of **5b**·0.76 $C_6H_6$ ·0.14H $_2$ O, **8b**·0.5 $C_6H_6$ ·0.125H $_2$ O, (**8b**/**13**)· $C_6H_6$ ·0.25H $_2$ O, and **13**· $C_6H_6$ ·0.25H $_2$ O were not located. The crystal of **6b<sup>o</sup>** is a racemic twin with twin fractions in an almost equal ratio (0.53 : 0.47).

The crystallographic parameters and the X-ray diffraction data collection and refinement statistics are given in Tables 2–6. All calculations were carried out with the use of the SHELXTL-Plus program package.<sup>46</sup>

The atomic coordinates and other experimental data were deposited with the Cambridge Crystallographic Data Centre\*

with the CSD refcodes 778792 (**1b**), 778793 (**2b**), 778794 (**2b**/**11**), 778795 (**3b**·0.5 $C_6H_6$ ), 778796 (**4b**), 778797 (**4b**·0.5 $C_6H_6$ ), 778798 (**5b**), 778799 (**5b**·0.76 $C_6H_6$ ·0.14H $_2$ O), 778800 (**6b<sup>m</sup>**), 778801 (**6b<sup>o</sup>**), 778802 (**7b**·0.5 $C_6H_6$ ), 778803 (**8b**·0.5 $C_6H_6$ ·0.125H $_2$ O), 778804 ((**8b**/**13**)· $C_6H_6$ ·0.25H $_2$ O), 778805 (**13**· $C_6H_6$ ·0.25H $_2$ O), 778806 (**9b**·MeCN·0.5 $C_6H_6$ ·H $_2$ O), 778807 (**9b**·NH $_4$ ClO $_4$ ), and 778808 (**14**·NH $_4$ ClO $_4$ ·H $_2$ O).

This study was financially supported by the Russian Foundation for Basic Research (Project No. 11-03-00647), the Royal Society of the UK (L. G. Kuz'mina and J. A. K. Howard), the Royal Society of Chemistry of the UK (L. G. Kuz'mina and A. V. Churakov, Grants for Foreign Authors), and the Photochemistry Center of the Russian Academy of Sciences.

## References

1. L. G. Kuz'mina, A. I. Vedernikov, N. A. Lobova, S. K. Sazonov, S. S. Basok, J. A. K. Howard, S. P. Gromov, *Izv. Akad. Nauk, Ser. Khim.*, 2009, 1161 [*Russ. Chem. Bull., Int. Ed.*, 2009, **58**, 1192].
2. J. L. R. Williams, *J. Org. Chem.*, 1960, **25**, 1839.
3. G. J. M. Schmidt, *J. Pure Appl. Chem.*, 1971, **27**, 647.
4. *Einführung in die Photochemie*, Ed. H. G. O. Becker, VEB Deutscher Verlag der Wissenschaften, Berlin, 1976.
5. V. Ramamurthy, K. Venkatesan, *Chem. Rev.*, 1987, **87**, 433.
6. S. R. Marder, J. W. Perry, B. G. Tiemann, R. E. Marsh, W. P. Schaefer, *Chem. Mater.*, 1990, **2**, 685.
7. C.-H. Huang, D. M. Bassani, *Eur. J. Inorg. Chem.*, 2005, 4041.
8. M. Nagarathinam, J. J. Vittal, *Macromol. Rapid Commun.*, 2006, **27**, 1091.
9. J. Svoboda, B. König, *Chem. Rev.*, 2006, **106**, 5413.
10. S. P. Gromov, *Izv. Akad. Nauk, Ser. Khim.*, 2008, 1299 [*Russ. Chem. Bull., Int. Ed.*, 2008, **57**, 1325].
11. N. Hoffmann, *Chem. Rev.*, 2008, **108**, 1052.
12. F. Li, J. Zhuang, G. Jiang, H. Tang, A. Xia, L. Jiang, Y. Song, Y. Li, D. Zhu, *Chem. Mater.*, 2008, **20**, 1194.
13. L. R. MacGillivray, *CrystEngComm*, 2002, **4**, No. 7, 37.
14. I. Turowska-Tyrk, *J. Phys. Org. Chem.*, 2004, **17**, 837.
15. F. H. Allen, M. F. Mahon, P. R. Raithby, G. P. Shields, H. A. Sparkes, *New J. Chem.*, 2005, **29**, 182.
16. T. Friscic, L. R. MacGillivray, *Supramol. Chem.*, 2005, **17**, 47.
17. D.-K. Bukar, G. S. Papaefstathiou, T. D. Hamilton, Q. L. Chu, I. G. Georgiev, L. R. MacGillivray, *Eur. J. Inorg. Chem.*, 2007, 4559.
18. L. R. MacGillivray, *J. Org. Chem.*, 2008, **73**, 3311.
19. L. R. MacGillivray, G. S. Papaefstathiou, T. Friscic, T. D. Hamilton, D.-K. Busar, Q. Chu, D. B. Varshney, I. G. Georgiev, *Acc. Chem. Res.*, 2008, **41**, 280.
20. A. I. Vedernikov, S. P. Gromov, N. A. Lobova, L. G. Kuz'mina, Yu. A. Strelenko, J. A. K. Howard, M. V. Alfimov, *Izv. Akad. Nauk, Ser. Khim.*, 2005, 1896 [*Russ. Chem. Bull., Int. Ed.*, 2005, **54**, 1954].
21. S. P. Gromov, A. I. Vedernikov, N. A. Lobova, L. G. Kuz'mina, S. N. Dmitrieva, O. V. Tikhonova, M. V. Alfimov, *Pat. RF 2278134; Byul. Izobret. [Inventor Bull.]*, 2006, No. 17 (in Russian).

\* CCDC, 12 Union Road, Cambridge CB21EZ, UK (fax: (+44)1223 33 6033; e-mail: deposit@ccdc.cam.ac.uk). The data can also be obtained from the authors.

22. L. G. Kuz'mina, A. I. Vedernikov, N. A. Lobova, A. V. Churakov, J. A. K. Howard, M. V. Alfimov, S. P. Gromov, *New J. Chem.*, 2007, **31**, 980.
23. A. I. Vedernikov, L. G. Kuz'mina, S. K. Sazonov, N. A. Lobova, P. S. Loginov, A. V. Churakov, Yu. A. Strelenko, J. A. K. Howard, M. V. Alfimov, S. P. Gromov, *Izv. Akad. Nauk, Ser. Khim.*, 2007, 1797 [*Russ. Chem. Bull., Int. Ed.*, 2007, **56**, 1860].
24. L. G. Kuz'mina, A. I. Vedernikov, S. K. Sazonov, N. A. Lobova, P. S. Loginov, J. A. K. Howard, M. V. Alfimov, S. P. Gromov, *Kristallografiya*, 2008, **53**, 460 [*Crystallogr. Repts (Engl. Transl.)*, 2008, **53**, 428].
25. L. G. Kuz'mina, A. I. Vedernikov, J. A. K. Howard, M. V. Alfimov, S. P. Gromov, *Ross. Nanotekh.*, 2008, **3**, No. 7–8, 32 [*Nanotechnologies in Russia (Engl. Transl.)*, **3**, 408].
26. J. L. R. Williams, S. K. Webster, J. A. Van Allan, *J. Org. Chem.*, 1961, **26**, 4893.
27. F. H. Quina, D. G. Whitten, *J. Am. Chem. Soc.*, 1977, **99**, 877.
28. A. Takagi, B. R. Suddaby, S. L. Vadas, C. A. Backer, D. G. Whitten, *J. Am. Chem. Soc.*, 1986, **108**, 7865.
29. H. Usami, K. Takagi, Y. Sawaki, *J. Chem. Soc., Faraday Trans.*, 1992, **88**, 77.
30. W.-Q. Zhang, J.-P. Zhuang, C.-B. Li, H. Sun, X.-N. Yuan, *Chin. J. Chem.*, 2001, **19**, 695.
31. W. Zhang, G. Shen, J. Zhuang, P. Zheng, X. Ran, *J. Photochem. Photobiol. A: Chem.*, 2002, **147**, 25.
32. H.-X. Li, L.-Z. Wu, L.-P. Zhang, C.-H. Tung, *Org. Lett.*, 2002, **4**, 1175.
33. S. Yamada, N. Uematsu, K. Yamashita, *J. Am. Chem. Soc.*, 2007, **129**, 12100.
34. H. Shayira Banu, A. Lalitha, K. Pitchumani, C. Srinivasan, *Chem. Commun.*, 1999, 607.
35. M. Pattabiraman, A. Natarajan, R. Kaliappan, J. T. Mague, V. Ramamutthy, *Chem. Commun.*, 2005, 4542.
36. R. Kaliappan, L. S. Kaanumalle, A. Natarajan, V. Ramamutthy, *Photochem. Photobiol. Sci.*, 2006, **5**, 925.
37. R. Kaliappan, M. V. S. N. Maddipatla, L. S. Kaanumalle, V. Ramamutthy, *Photochem. Photobiol. Sci.*, 2007, **6**, 737.
38. M. V. S. N. Maddipatla, L. S. Kaanumalle, A. Natarajan, M. Pattabiraman, V. Ramamutthy, *Langmuir*, 2007, **23**, 7545.
39. M. Horner, S. Hünig, *J. Am. Chem. Soc.*, 1977, **99**, 6120.
40. J. Harada, K. Ogawa, *J. Am. Chem. Soc.*, 2004, **126**, 3539.
41. J. Harada, K. Ogawa, *Chem. Soc. Rev.*, 2009, **38**, 2244.
42. S. K. Kearsley, *Studies in Organic Chemistry. 32. Organic Solid State Chemistry*, Ed. G. R. Desiraju, Elsevier, Amsterdam, 1987, p. 69.
43. F. H. Allen, *Acta Crystallogr., Sect. B*, 2002, **58**, 380.
44. S. P. Gromov, N. A. Lobova, A. I. Vedernikov, L. G. Kuz'mina, J. A. K. Howard, M. V. Alfimov, *Izv. Akad. Nauk, Ser. Khim.*, 2009, 1179 [*Russ. Chem. Bull., Int. Ed.*, 2009, **58**, 1211].
45. *SAINT*, Version 6.02A, Bruker AXS Inc., Madison, Wisconsin (USA), 2001.
46. *SHELXTL-Plus*, Version 5.10, Bruker AXS Inc., Madison, Wisconsin (USA), 1997.

Received June 11, 2010;  
in revised form May 25, 2011